Lysozyme Degradation by Azo Initiator AAPH, Fenton Reaction, and Ionizing Radiation

By
Simon Hung Tran

Submitted to the graduate degree program in Pharmaceutical Chemistry and the Graduate Faculty of the University of Kansas in partial fulfillment of the requirements for the degree of Master of Science.

_____
Chairperson Christian Schöneich
Chair, Pharmaceutical Chemistry

_____
John F. Stobaugh
Associate Dean of Research and Graduate Affairs

_____
Cindy Wu
Associate Director, Allergan

Date Defended: 06/26/2017

The Thesis Committee for Simon Hung Tran

certifies that this is the approved version of the following thesis:

LYSOZYME DEGRADATION BY AZO INITIATOR AAPH, FENTON REACTION, AND IONIZING RADIATION

_____

Chairperson Christian Schöneich

Date approved: 06/26/2017

Abstract

Oxidant generators, such as 2,2'-azobis(2-amidinopropane) dihydrochloride (AAPH) and the Fenton reaction, have been used to elucidate protein oxidation pathways and subsequently to screen for stabilizers that could prevent potential damage to the protein of interest. The current study evaluated the use of AAPH and the Fenton reaction as forced degradation tools to simulate the effect of terminal sterilization by ionizing radiation using the model protein lysozyme. The results indicate that when the protein is stressed to the same level as the irradiation process, the damage to the protein caused by the stress conditions is different than that caused by the actual irradiation process. In this work, protein aggregation was determined to be the main degradation pathway for the irradiated lysozyme powder. In contrast, oxidation was found to be the main degradation pathway for the lysozyme solution stressed with AAPH and the Fenton reaction. Since the main degradation pathways are different, the use of AAPH or the Fenton reaction as a surrogate for the irradiation process may not be effective for screening protein stabilizers.

Acknowledgements

I wish to acknowledge my research advisor, Dr. Christian Schoneich, Takeru Higuchi Distinguished Professor at The University of Kansas, for his guidance and critical input into the research. In addition, I would to thank my colleagues at Allergan for their wholehearted support: Dr. Cindy Wu for being my onsite advisor, Dr. James Cunningham for his encouragement and scientific resources, and Dr. Patrick Hughes for his sponsorship of the program. This work is supported in part by The Allergan Tuition Assistance Program.

TABLE OF CONTENTS

LIST OF TABLES

LIST OF FIGURES

CHAPTER I: INTRODUCTION

Background and Significance

The Food and Drug Administration (FDA) requires that all sterile injectable pharmaceutical products have a Sterility Assurance Level (SAL) of 10^{-6} or better using a pharmaceutically acceptable terminal sterilization process, such as sterile filtration, heat sterilization, gaseous sterilization, and irradiation (1). For solid dosage forms of protein-loaded, sustained-release pharmaceutical products, such as polymeric implants and microparticles, irradiation is typically the most feasible method of sterilization. However, irradiation using gamma rays as the source can potentially cause detrimental damage to most proteins through chemical and physical modifications (2–6). Therefore, prior to implementing the sterilization process of gamma irradiation, it is crucial to perform stability and forced degradation studies to evaluate the limitation of the protein of interest under such oxidative stress.

One of the forced degradation methods typically used to evaluate protein oxidation by radicals is the Fenton reaction. Invented in the 1890s by Henry John Horstman Fenton, the Fenton reaction is composed of hydrogen peroxide and iron, which form hydroxyl radicals after mixing (7). Although the Fenton reaction can generate hydroxyl radicals to deliberately oxidize the protein of interest, there is uncertainty about using such a system exclusively to evaluate and stabilize a protein being exposed to ionizing radiation. In a comparative study done by Edwards et al., the authors suggested that although the inactivation level of the model protein lysozyme is the same for both the gamma irradiation and the Fenton reaction, the mechanism of action is seemingly different for the two processes (6).

Another class of compounds that is being used for the deliberate oxidation of proteins is the azo initiators. Azo initiators are compounds that thermally decompose and react with oxygen to form peroxyl radicals with predictable stoichiometry (8,9). Similar to the Fenton reaction, the oxidation of proteins by the azo initiators seems to be selective or site-specific as opposed to the gamma irradiation where the effect is less selective (6,10). While the azo compounds have been used to model oxidation of proteins by peroxyl radicals (10–12), it is still indeterminate whether the resulting degradation is comparable to the degradation observed from the gamma irradiation using the standard protocol employed by the pharmaceutical industry.

To address the validity of the use of the forced degradation methods to simulate the effect of ionizing radiation, the current research directly compares the degradation patterns of a model protein, lysozyme, caused by gamma irradiation in the solid state to that caused by the radicals derived from the azo initiator AAPH and the Fenton reaction in an aqueous solution. The contribution of this study could give more insights to whether the use of the azo initiator AAPH and the Fenton reaction is valid as a screening tool to identify stabilizing agents against ionizing radiation.

The Properties of Lysozyme

Lysozyme from hen egg-white is comprised of a single polypeptide chain of 129 amino acids with a molecular weight of 14,313 g/mol. With 4 intramolecular disulfide bonds, the polypeptide chain folds into an ellipsoidal shape with the dimensions 45 x 30 x 30 Å (13). Figure 1 displays the positions of the disulfide bonds within the lysozyme primary sequence. Based on the primary sequence, the molar absorption coefficient (extinction coefficient) of lysozyme was determined to be 2.65 AU*(ml/mg)$^{-1}$*cm^{-1} using the method from Pace et al. 1995 (14). The isoelectric point of the protein was determined previously to be pH 11 by Rezwan et al. 2005 (15).

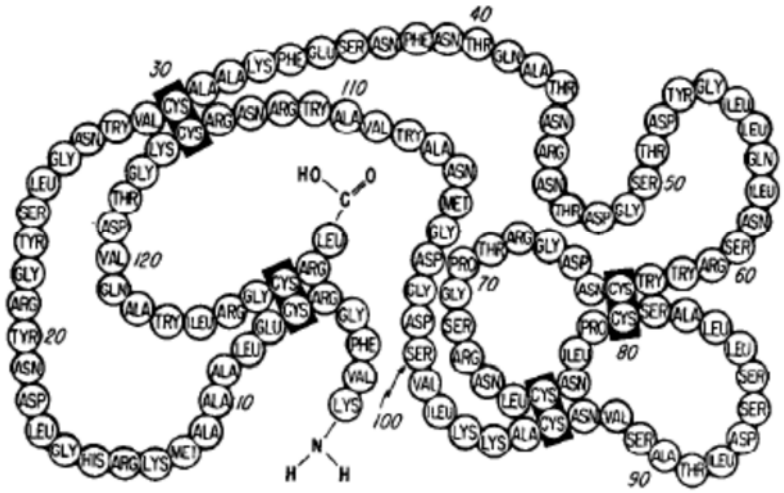

Figure 1 – The primary sequence of hen egg-white lysozyme showing the locations of the 4 disulfide bonds, reproduced from Canfield and Liu 1965 with permission (16).

The Gamma Irradiation Process

Gamma irradiation is the process of exposing pharmaceutical products and medical devices along with other healthcare products to gamma rays, a type of ionizing radiation that can cause propagandized ionization. Gamma rays emitted from sources such as radioactive isotope Cobalt-60 (^{60}Co) contains about 1-2 MeV of energy that can penetrate matter to break chemical bonds, such as those in the bacterial deoxyribonucleic acid (DNA), effectively inhibiting the bacterial division and growth (17).

Radiation dosage is measured in gray or kilogray using the dosimeters, which are calibrated and traceable to a national standard. The applied dose is dependent on the rate and the exposure time, that the product is in the irradiation chamber, which can take minutes to hours. The typical minimum dose is 25kGy, which was set previously to meet the SAL (17).

CHAPTER II: METHODS

The Gamma Irradiation Process of Lysozyme Solid Powder

Lysozyme powder (hen egg white, >90% protein, >40,000units/mg, Sigma, Cat # L6876) was weighed into individual vials, which were then vacuum-dried for 2 hours at room temperature at 100 mTorr in a LyoStar II lyophilizer to remove residual water. The vials were sealed under vacuum and divided into 2 groups, the irradiation group and the non-irradiation group. The irradiation group was sent for gamma irradiation at Sterigenics (Corona, CA, USA) with a specified dose range of 25 – 40 kGy, the standard specified dosage. The actual delivered dose was determined from the dosimeters, which ranges from 30 kGy to 35 kGy. The non-irradiation group was stored at -20°C. This group includes the control (non-treated), the AAPH-treated group, and the Fenton-treated group.

Reversed-Phase Ultra Performance Liquid Chromatography

The reversed-phase ultra-performance liquid chromatography (RP-UPLC) was developed to assess changes to the protein hydrophobicity, resulting from chemical degradation and peptide fragmentation. The oxidation of the protein amino acid residues such as methionine, tryptophan, and tyrosine can modify the protein hydrophobicity, depending on the resulting conformation of the protein (18,19).

In a typical reversed-phase liquid chromatography experiment, the hydrophobicity of the molecule will determine the degree to which the molecule interacts with the hydrophobic stationary phase, which, normally, is an alkyl chain grafted onto a silica support packed into a cylinder column. The stronger the hydrophobic interaction between the molecule and the

stationary phase, the longer the molecule will retain on the column as a mobile phase with the opposite polarity passes through the column. This differences in retention time separate different molecules with varied hydrophobicity. However, there could be secondary interactions, such as ionic interaction and polar interaction, in addition to hydrophobic interaction that could affect the retention time of the molecules (20). Therefore, it is important to ensure that these secondary interactions do not interfere with the intended separation.

For the separation of different species of the native and modified lysozyme, a stationary phase composed of an 18-carbon alkyl chain (C_{18}) covalently bonded to a modified silica particle called polyethoxysilane, commercially referred to as Ethylene Bridged Hybrid (BEH) technology, was chosen due to its stability at a wide pH range and at high temperature (21). These particles, having a size distribution of around 1.7µm, were packed into a column with an inner diameter of 2.1mm and a length of 50mm.

To elute the protein from the column, a gradient of acetonitrile and water was used as the mobile phase. Trifluoroacetic acid (TFA) was added to both components of the mobile phase to suppress the secondary interactions caused by the residual silanol groups on the silica surface (20).

The method was optimized for gradient, temperature, and flow rate. The gradient rate was evaluated simultaneously with the baseline mobile phase composition. The baseline mobile phase composition coats the column with different percentages of acetonitrile at 10%, 15%, 20%, and 25%, masking the column hydrophobicity prior to the adsorption of the protein. Different

gradient rates of %B (10.0%B/min, 9.4%B/min, 8.9%B/min, and 8.3%B/min) then selectively elute the bound species of lysozyme from the column after the adsorption. Figure 2 shows the effect of the 4 conditions on the resolution of the 2 main peaks. The resolution values were calculated using the following resolution equation (Rs) from the United States Pharmacopoeia (USP):

$$R_S = 2(t_{R2} - t_{R1}) / (W1 + W2)$$

where t_{R2} and t_{R1} are the retention times of the 2 peaks of interest; and W1 and W2 are the corresponding tangent widths of the peaks. The condition with 20% baseline and a rate of 8.9%B/min was chosen with the rationale that less acetonitrile is needed to achieve the same effect as the condition of 25% baseline with a rate of 8.3%B/min.

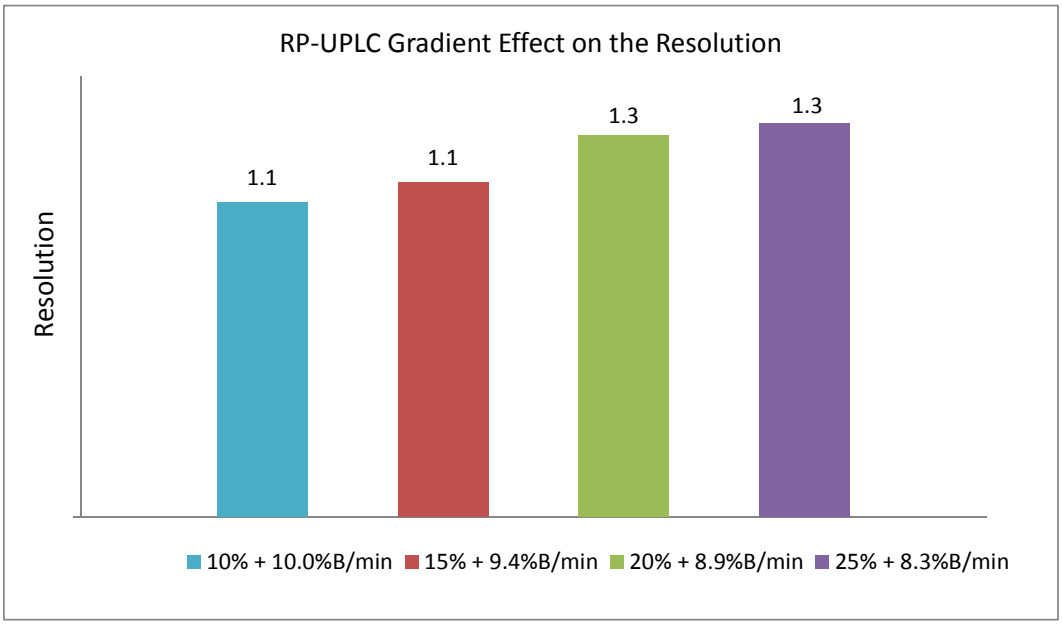

Figure 2 – RP-UPLC gradient effect on the resolution of the 2 main peaks

To evaluate the efficiency of different flow rates, a reduced Van Deemter curve was constructed using a volumetric flow rate of 0.2mL/min, 0.5mL/min, and 0.8mL/min. The reduced Van Deemter curve is a plot of the reduced plate height (h) against the reduced velocity (ν) based on the Van Deemter equation:

$$H = A + B/u + Cu$$

where H is the plate height, derived from the theoretical plates (N) divided by the column length (L); the A-term is determined by the eddy diffusion; the B-term is determined by the longitudinal molecular diffusion; the C-term is determined by the mass transfer effect; and u is the linear velocity (22). The following equations were used for the Van Deemter curve:

$$\nu = D_m/d_P$$

$$h = H / d_P$$

$$\nu = u/v$$

where v is the diffusion velocity; D_m is the diffusion coefficient of lysozyme; d_P is the silica particle size; h is the reduced plate height; ν is the reduced velocity. As described previously, the column dimension is composed of 50mm length, 2.1mm inner diameter, and 1.7μm particle size. A diffusion coefficient (D_m) of 10^{-6} cm^2/s was used for lysozyme (23).

The reduced Van Deemter curve displayed in Figure 3 shows that there was no change observed in the reduced height as the reduced velocity increases, indicating no loss in efficiency. Although there was no change in efficiency, the resolution was improved slightly as the flow rate increases (Figure 4). Since the flow rate of 0.8mL/min achieved the highest resolution without affecting efficiency, it was chosen as the flow rate of the method.

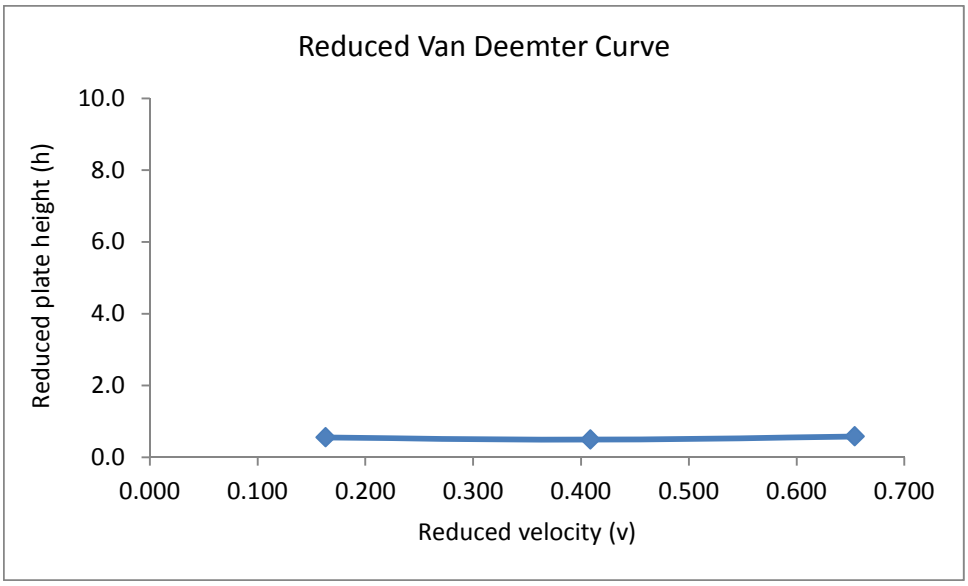

Figure 3 – Reduced Van Deemter curve from the RP-UPLC analysis of lysozyme.

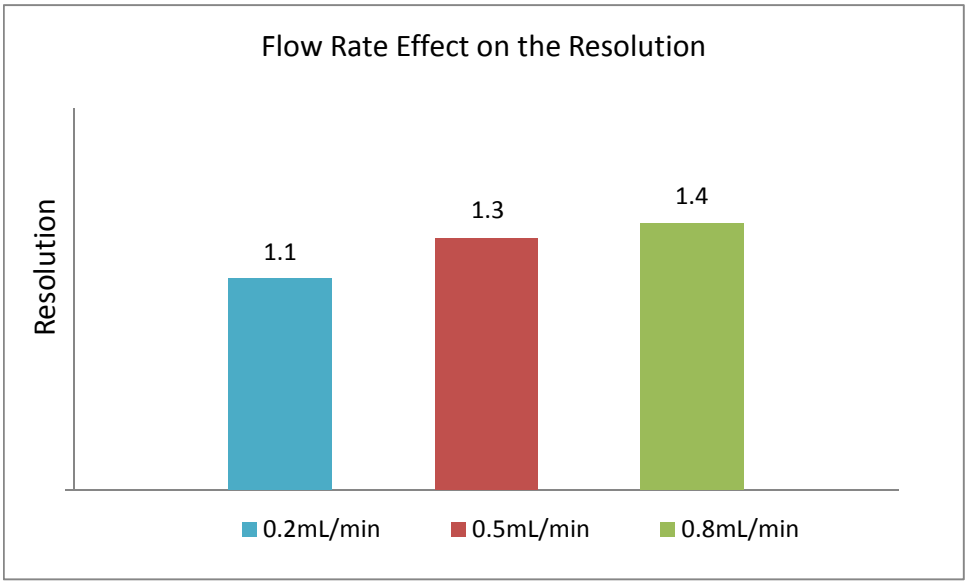

Figure 4 – RP-UPLC flow rate effect on the resolution of the 2 main peaks

Column temperature could affect the selectivity of the column, and, therefore, it was evaluated at 25°C, 35°C, and 45°C. Figure 5 confirms that the selectivity of the column was positively changed to show an improvement in resolution as the column temperature increased from 25°C to 45°C. Due to favorable increase in resolution, the column temperature of 45°C was chosen.

The final method conditions are listed in Table 1, and a representative chromatogram is shown in Figure 6.

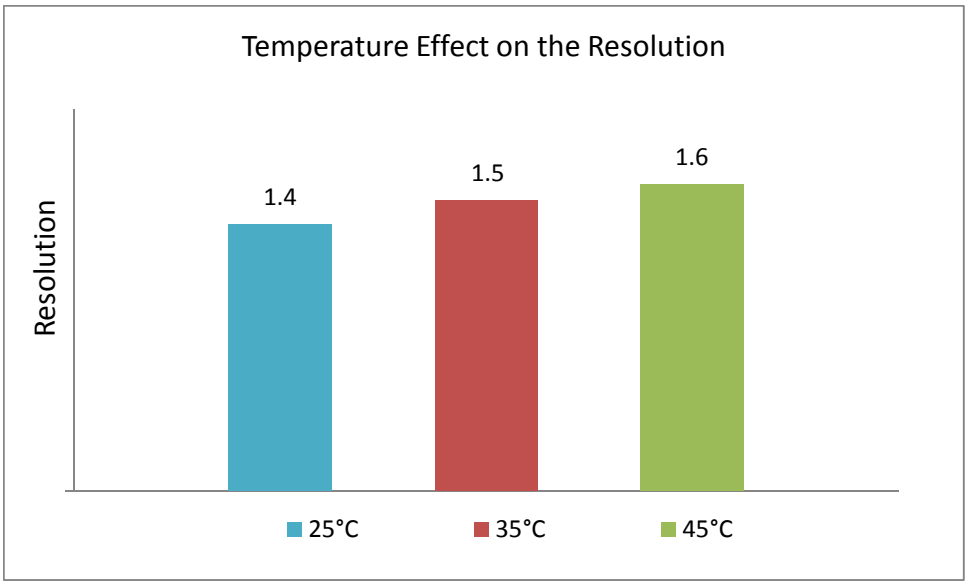

Figure 5 – The effect of column temperature on the resolution of the 2 main peaks of lysozyme for the RP-UPLC method.

Table 1 – Final RP-UPLC Method Conditions for the Analysis of Lysozyme

HPLC System:	Waters Acquity	
Column:	Acquity UPLC BEH C18, 1.7µm, 2.1x50mm, Part# 186002350	
Column Temp:	45°C	
Mobile Phase A:	0.1% TFA in water	
Mobile Phase B:	0.1% TFA in acetonitrile	
Flow rate:	0.8ml/min	
Detection:	UV @ 280nm	
Extinction Coefficient:	2.65 AU*(ml/mg)$^{-1}$*cm^{-1}	
Injection Volume:	2µL-20µL	
Gradient:		
Time (min)	Mobile Phase A	Mobile Phase B
0.00 (initial)	80	20.0
0.50 (equilibration)	80	20.0
5.50 (separation)	36	64.0
6.00 (washing)	0	100.0
6.02 (equilibration)	80	20.0
7.50 (equilibration)	80	20.0

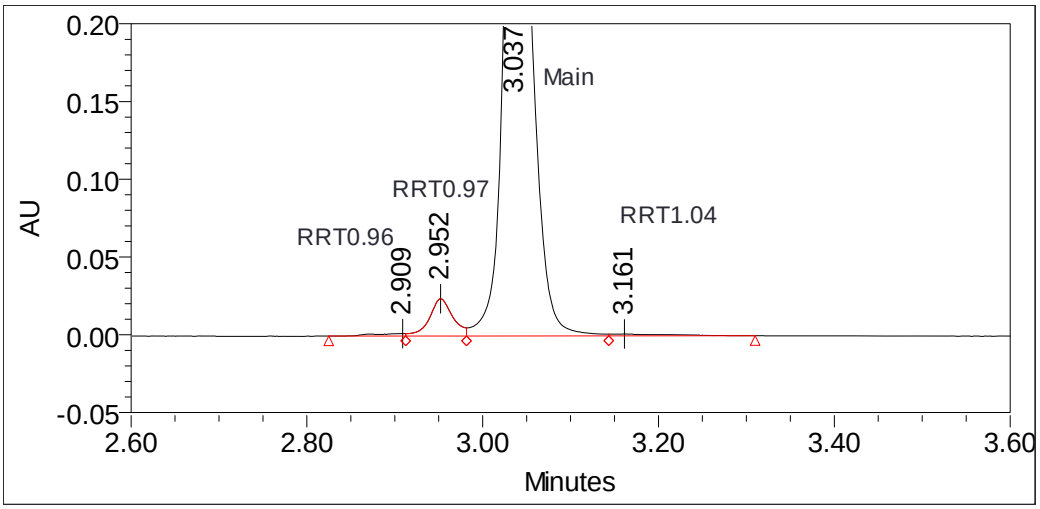

Figure 6 – Representative RP-UPLC chromatogram of a 1mg/ml lysozyme in 10mM phosphate pH7.4 using the final method conditions in Table 1.

Size Exclusion Chromatography

Size Exclusion Chromatography (SEC) is a form of liquid chromatography that separates macromolecules based on their hydrodynamic sizes. The main principle of retention in SEC is the resistance to flow or diffusion of the molecules through a column using pores of different sizes. Packed in a cylinder column are particles with pores designed to limit the flow of the molecules of interest through the column. Smaller molecules that fit inside the pores are retained on the column and thus, elute later than the larger molecules that do not fit inside the pores since the diffusion time of the smaller molecules are longer than that of the larger molecules. In contrast to the reversed-phase liquid chromatography method, in SEC, the interactions of the column resins were not intended to contribute to the retention of the molecules, and thus, such secondary interactions should be minimized if not eliminated allowing only the difference in diffusion as the sole separation method.

For the separation of lysozyme and its related species, a G2000SW$_{XL}$ from TOSOH Bioscience was chosen based on its 5µm silica particles with an average pore size of 12.5nm (125Å). This

column was designed to separate molecules with the molecular weights in the same range as lysozyme. The initial mobile phase was an aqueous solution of 20mM phosphate and 300mM sodium chloride with a pH of 6.7. The 300mM of sodium chloride was added to minimize the potential ionic interaction of lysozyme with the column. The chromatogram in Figure 7 shows that at a flow rate of 0.5mL/min, lysozyme was separated from its related, high-molecular-weight (HMW) species. However, there was significant tailing observed from the main peak indicating that there might be secondary interactions that may have contributed to the additional retention.

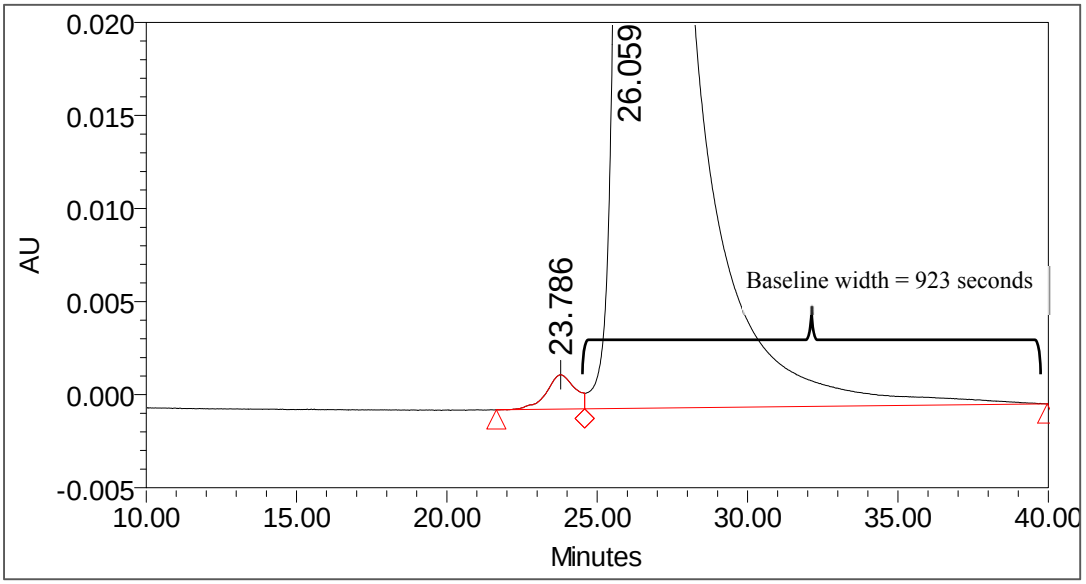

Figure 7 – SEC separation of lysozyme and its related species on a G2000SWxl with 20mM phosphate and 300mM sodium chloride at pH 6.7 as the mobile phase. The observed tailing of the main peak indicates that there are potential secondary interactions with the column.

Since 300mM of sodium chloride was already added to minimize the potential ionic interactions that lysozyme might have with the column, the observed tailing may have been the result of other secondary interactions, such as the hydrophobic interaction. Hydrophobic interaction was suspected since lysozyme hydrophobic amino acid residues, such as Val-2, Phe-3, Leu-17, Phe-34, Leu-75, and Trp-123, were on the surface of the protein rather than buried in the core of its native conformation (6,13). Thus, to reduce the hydrophobic interaction, 10% of acetonitrile were added to the initial mobile phase composed of 20mM phosphate and 300mM sodium chloride. The chromatogram in Figure 8 shows that the retention time of the main peak shifted from 26.1 minutes (Figure 7) to 22.8 minutes (Figure 8) and that the peak tailing effect was improved with the addition of 10% acetonitrile. The shifting of the main peak retention time to the left with the addition of 10% acetonitrile indicates that there are hydrophobic interactions between the silica particles and lysozyme that contributed to the additional retention time of the protein. The addition of 20% acetonitrile improved the peak tailing effect slightly further with a slight shift in retention time to the left as shown in Figure 9. The chromatogram in Figure 10 shows that the addition of 30% acetonitrile increased the peak area of the HMW species while shifting the retention time to the right, which is opposite of the trend observed previously. This may be the result of the mobile phase effect on the protein physical stability, leading to method-induced artifacts.

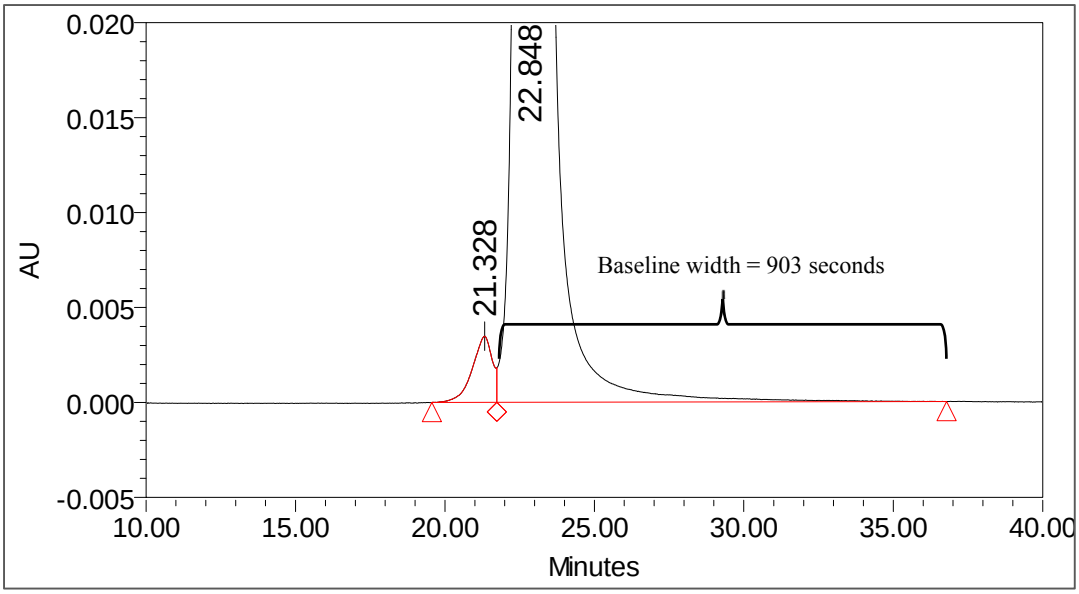

Figure 8 – SEC separation of lysozyme and its related species on a G2000SW$_{xl}$ with 20mM phosphate, 300mM sodium chloride, and 10% acetonitrile at pH 6.7 as the mobile phase. Peak tailing was still noticeable with the addition of 10% acetonitrile.

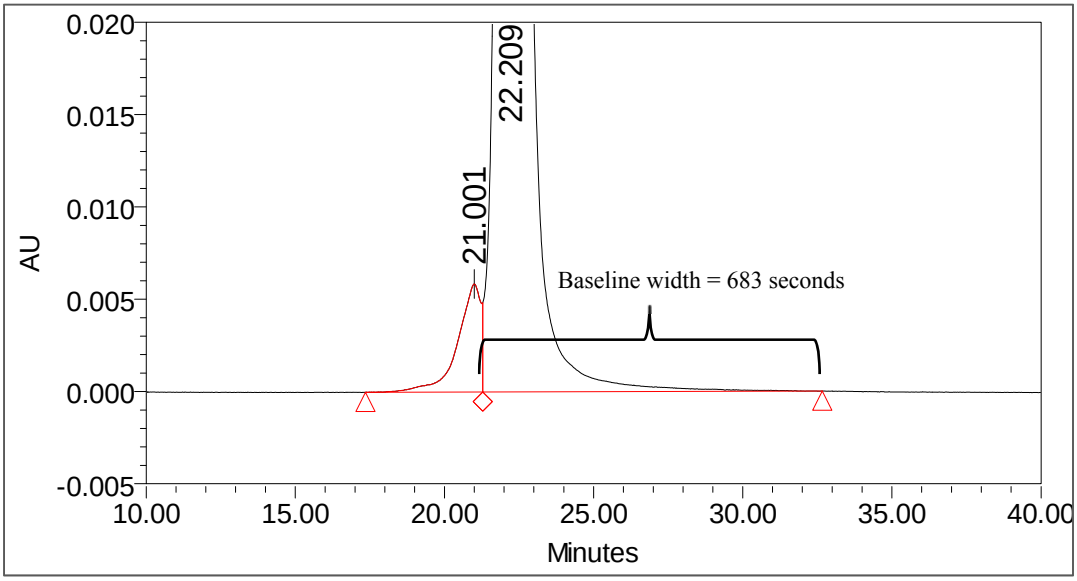

Figure 9 – SEC separation of lysozyme and its related species on a G2000SWxl with 20mM phosphate, 300mM sodium chloride, and 20% acetonitrile at pH 6.7 as the mobile phase. Peak tailing was still noticeable with the addition of 20% acetonitrile.

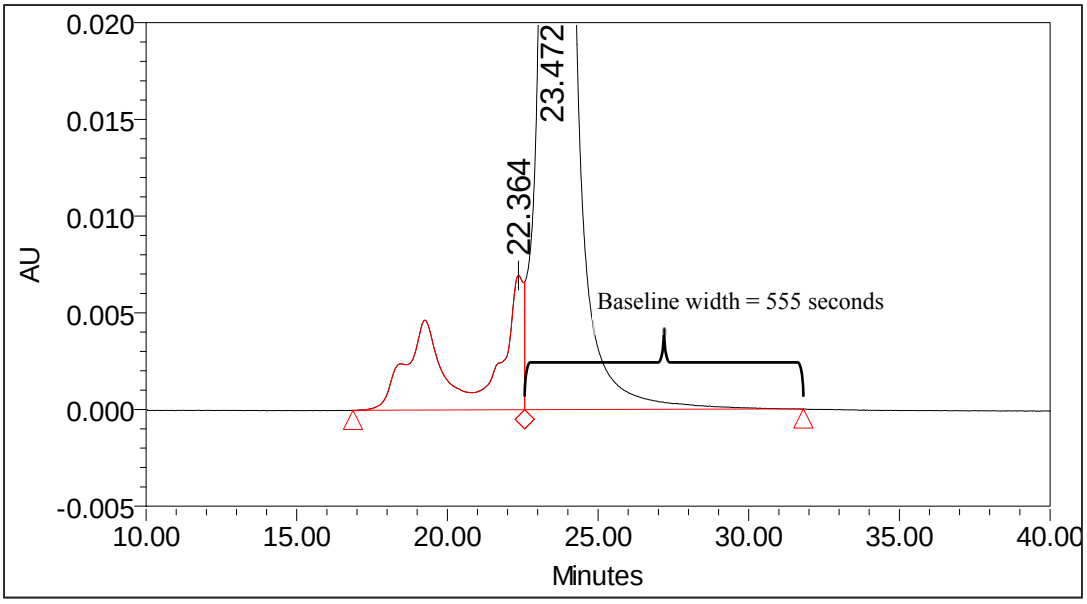

Figure 10 – SEC separation of lysozyme and its related species on a G2000SWxl with 20mM phosphate, 300mM sodium chloride, and 30% acetonitrile at pH 6.7 as the mobile phase. Peak tailing was minimized, but the mobile phase may have caused unintended instability of lysozyme as observed in the increase in the high molecular weight peak.

To minimize the effect of peak tailing without producing method-induced artifacts, acetonitrile was replaced with isopropyl alcohol (IPA). Additionally, the pH of the mobile phase was changed to 4 from 6.7 to minimize the effect of disulfide exchange (see Chapter III) by adding 0.1% phosphoric acid to the mobile phase. The final mobile phase composition is 20mM phosphate, 300mM sodium chloride, 10% IPA, and 0.1% phosphoric acid at pH 4. The chromatogram in Figure 11 shows that the retention time of the main peak shifted to the left (20.5 minutes versus 23.5 minutes when using 30% acetonitrile as the mobile phase additive in Figure 10). Baseline peak width decreased 3 folds, from 555 seconds to 177 seconds, a significant improvement. There was no increase in lysozyme HMW species observed.

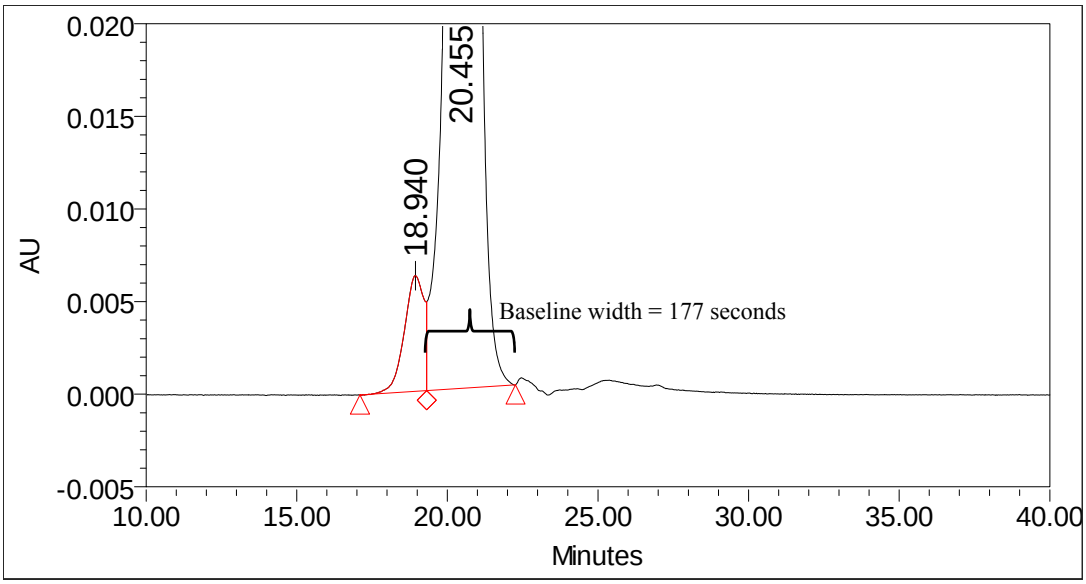

Figure 11 – SEC separation of lysozyme and its related species on a G2000SWxl with 20mM phosphate, 300mM sodium chloride, 10% isopropyl alcohol, 0.1% phosphoric acid at pH 4 as the mobile phase. Peak tailing was significantly minimized with no method-generated degradation.

The viscosity of IPA combined with the flow rate of 0.5mL/min caused a significant increase in the pressure drop for the system. The resulting system pressure is greater than the maximum operating pressure of 7.2 MPa, recommended by the column manufacturer. To decrease the effect of pressure drop on the column, the flow rate was decreased to 0.15mL/min from 0.5mL/min. The chromatogram in Figure 12 shows that the decrease in flow rate led to an increase in retention time and widening of the main peak as the peak width increased to 579 seconds from 177 seconds. The increase in the peak width is not attributed to the effect of secondary interaction since the increase spread symmetrically throughout the peak whereas the effect of peak tailing due to secondary interaction increased the peak width asymmetrically. There was no on-column degradation observed, indicating that 10% IPA is a suitable mobile phase additive for the SEC analysis of lysozyme. Table 2 lists the final conditions for the SEC analysis of lysozyme.

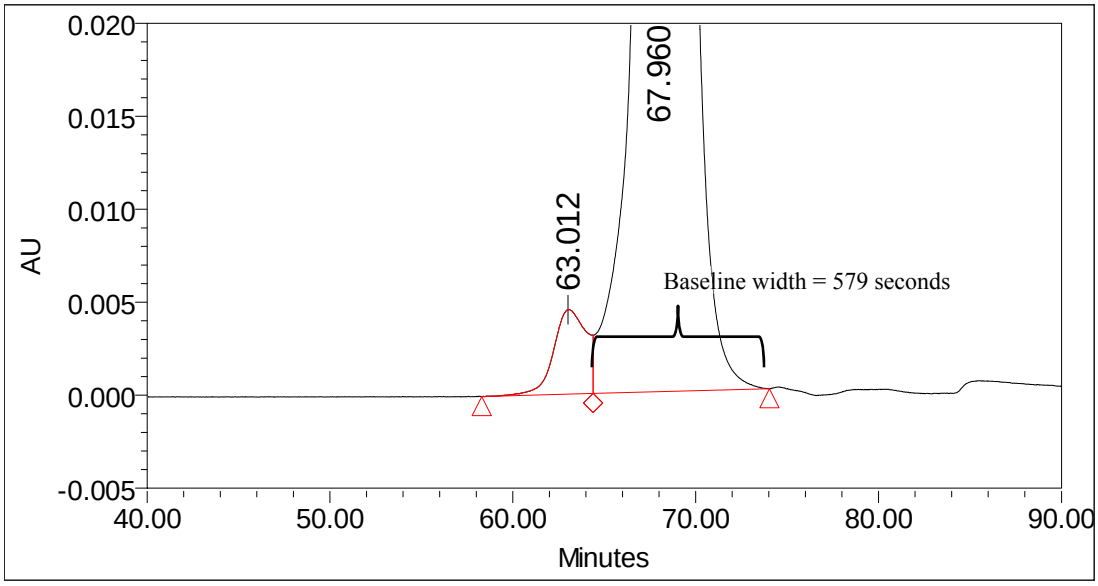

Figure 12 – SEC separation of lysozyme and its related species on a G2000SWxl with 20mM phosphate, 300mM sodium chloride, 10% isopropyl alcohol, 0.1% phosphoric acid at pH 4 as the mobile phase. The retention shifted to 68.0 minutes due to reduction in flow rate from 0.5mL/min to 0.15mL/min. Baseline peak width increased due to the increase in retention time.

Table 2 – Final SEC Method Conditions for the Analysis of Lysozyme

HPLC System:	Waters Alliance 2695
Column:	TOSOH TSK-GEL G2000SW$_{xl}$, 30x7.8mm, 5µm, Part # 08540
Column Temp:	Ambient
Mobile Phase:	20mM phosphate, 300mM sodium chloride, 10% IPA, 0.1% phosphoric acid, pH4
Flow rate:	0.15ml/min
Detection:	UV @ 280nm
Extinction Coefficient:	2.65 AU*(ml/mg)$^{-1}$*cm^{-1}
Injection Volume:	10µL
Isocratic Run Time:	100 minutes

Tryptophan Analysis

A primary amino acid residue of lysozyme and other proteins, such as parathyroid hormone, that is affected by oxidation via AAPH, the Fenton reaction, and ionizing radiation is tryptophan (6,10), and therefore, the analysis of tryptophan is crucial to support the comparison between these oxidation mechanisms. Tryptophan can be analyzed using the second derivative of the absorbance spectra at 288nm in 0.1M potassium hydroxide (24). However, the limitations for this method include interference from tyrosine, interference from iron(II) sulfate and hydrogen peroxide, and the required denaturation of the protein (6,24).

Tryptophan can be selectively hydrolyzed from the protein primary sequence and analyzed as a free amino acid using the hydrolysis method from Nakazawa and Manabe 1992 (25). To hydrolyze tryptophan from the protein, the authors used 3M of 2-mercaptoethanesulfonic acid vapor in a vacuum at 176°C for 25 minutes. However, the authors in Nakazawa and Manabe 1992 used a post-column derivatization HPLC method for the subsequent amino acid analysis. The authors in Sultana et al. 2012 show that it is possible to directly analyze the free tryptophan without derivatization (26) since tryptophan has an ultraviolet absorbance at 280nm with an extinction coefficient of 5,500 M^{-1} cm^{-1} (14).

In the current study, tryptophan was hydrolyzed from lysozyme using the method adapted from Nakazawa and Manabe 1992 with a slight modification in duration at 15 minutes instead of 25 minutes. To analyze the hydrolyzed tryptophan, a modified liquid chromatography (LC) method adapted from Sultana et al. 2012 was developed and qualified. The LC method is a RP-UPLC method utilizing a 1.7µm, BEH C18 Phenyl column with an inner diameter of 2.1mm and a length of 50mm. The mobile phase is composed of 90% of water, 10% of acetonitrile, and 0.1%

TFA to lower the pH to about 2. Table 3 lists the final RP-UPLC conditions for the analysis of the free tryptophan. Figure 13 displays the representative chromatogram of a tryptophan solution at 10µg/mL in water.

Table 3 – Final RP-UPLC Method Conditions for the Analysis of Tryptophan

HPLC System:	Waters Acquity
Column:	Acquity BEH C18 Phenyl, 1.7µm, 2.1x50mm, Part # 186002884
Column Temp:	25°C
Mobile Phase:	90% water, 10% acetonitrile, 0.1% TFA
Flow rate:	0.2mL/min
Detection:	UV @ 276nm
Extinction Coefficient:	26.93 AU*(ml/mg)$^{-1}$*cm^{-1}
Injection Volume:	2µL-20µL
Isocratic Run Time:	10 minutes

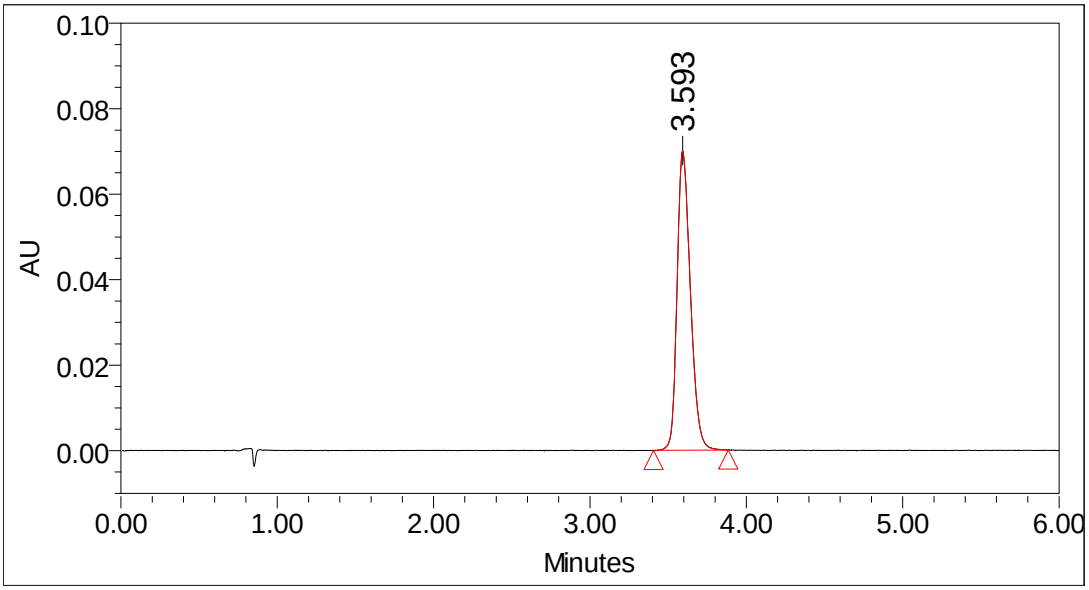

Figure 13 – Representative RP chromatogram of a 10µg/ml (49pmol/µL) tryptophan in water

The method was evaluated for linearity, sensitivity, and precision. Linearity was evaluated in the range of 1.0µg/mL (4.9nmol/ml) to 20µg/ml (97.9nmol/ml). Figure 14 shows that the area responses of the free tryptophan are linear in the evaluated concentration range with a correlation coefficient R^2 of 0.997. For sensitivity, the signal to noise (S/N) ratio method was used to determine the limit of detection (LOD) and limit of quantitation (LOQ). LOD is defined at the S/N ratio of 3, and LOQ is defined at the S/N ratio of 10. Based on the signal (height response) in the linearity range, the LOD and LOQ concentrations were determined to be 0.06µg/ml (0.3nmol/ml) and 0.20µg/ml (1.0nmol/ml), respectively. At 0.3nmol/ml, the detection limit is about 167 fold lower than the lowest concentration (50nmol/ml) of the linear range of the second derivative spectroscopy method (24).

The precision of the tryptophan analysis method includes the hydrolysis of the protein in addition to the analysis of the free tryptophan. About 0.1mg of lysozyme was hydrolyzed in the vapor phase 3M of 2-mercaptoethanesulfonic acid (MESA) at 176°C for 15 minutes. The resulting hydrolysates were analyzed by the RP-UPLC method directly and immediately after a 30-minutes cooling period. The analysis was done in triplicates using 3 different sample preparations. Table 5 shows the results of the recovery of tryptophan from the protein hydrolysis and the precision of the method. The recovery is in line with the findings from Nakazawa and Manabe at 95% (25), and the precision is at 2% RSD. The results show that the method is suitable for the analysis of tryptophan.

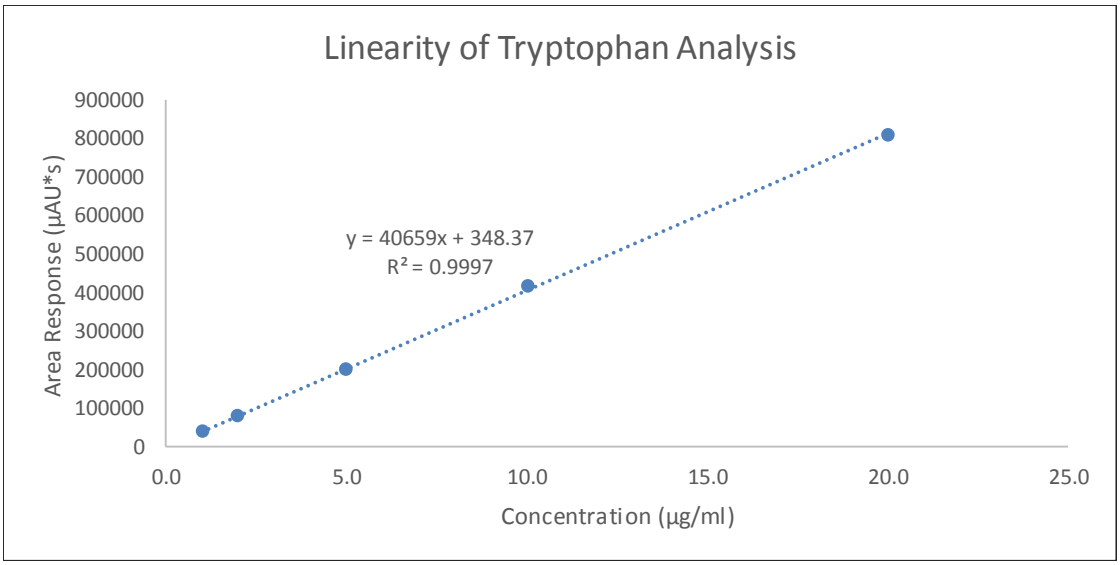

Figure 14 – Linearity of tryptophan analysis in the range of 1-20µg/ml

Table 4 – Sensitivity of the RP-UPLC Method for the Analysis of Free Tryptophan

Sample	Conc (µg/ml)	Height (µAU)	Noise (µAU)	S/N Ratio	LOD (µg/ml)	LOQ (µg/ml)
Trp 1µg/ml	1.00	7272	140	52	0.06	0.19
Trp 2µg/ml	2.00	14333	140	102	0.06	0.20
Trp 5µg/ml	5.00	35172	140	251	0.06	0.20
Trp 10µg/ml	10.00	70125	140	501	0.06	0.20
Trp 20µg/ml	20.00	125696	140	898	0.07	0.22
				Average (n=5)	0.06	0.20
				Standard Deviation (n=5)	0.004	0.012

Table 5 – The Recovery and Precision of the Tryptophan Analysis Method

Sample	Theo Trp (µg/ml)	Measured Trp (µg/ml)	Recovery (%)	Average (%)	Std Dev (%)	%RSD
Hydrolyzed Trp P1	9.1	8.5	93.1	94.8	1.9	2.0
Hydrolyzed Trp P2	8.6	8.1	94.5			
Hydrolyzed Trp P3	9.6	9.3	96.7			

CHAPTER III: RESULTS & DISCUSSION

Lysozyme Chemical Stability

Lysozyme is susceptible to oxidation with high concentrations of hydrogen peroxide, which typically oxidize the accessible methionine and tryptophan residues on the protein (11). This result was derived from a lysozyme stress study with hydrogen peroxide. The reaction conditions of the study comprised of 1mg/ml lysozyme, three concentrations of hydrogen peroxide (1%, 2%, and 3% w/w), and a duration of 60 minutes. The study was carried out at room temperature. As shown in the normalized chromatogram in Figure 15, all major degradation peaks increase in concentration as the concentration of hydrogen peroxide increases. The dose-response effect of hydrogen peroxide is shown in Figure 16. The results demonstrated that lysozyme is sensitive to oxidation and that the oxidation products can be detected using the RP-UPLC method. Due to the chemical instability of the protein to relatively simple oxidation, lysozyme is a good model protein to study protein oxidation.

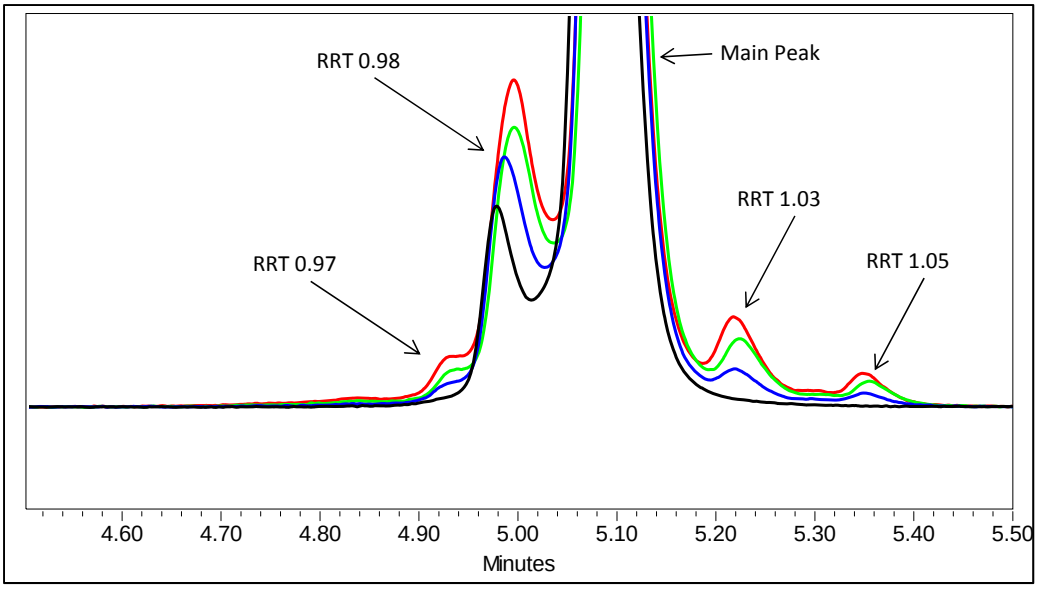

Figure 15 – Normalized, overlaid chromatogram of 1mg/ml lysozyme stressed with hydrogen peroxide at 0% (Black), 1% (Blue), 2% (Green), and 3% (Red). There was a steadily increase in the lysozyme degradation peaks as the concentration of hydrogen peroxide increases.

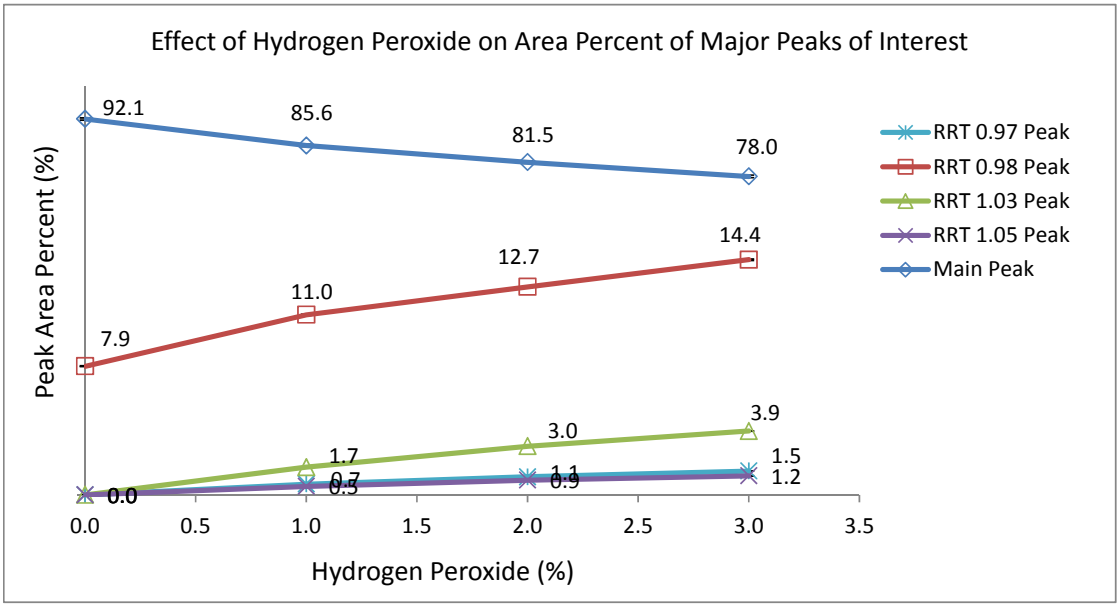

Figure 16 – The effect of hydrogen peroxide on the area percent of the major peaks of interest of lysozyme. Error bars based on the standard deviations are present (n=3). Standard deviation ranges from 0.1 – 0.3%.

The degradation of lysozyme in an acidic environment was not observed, indicating that lysozyme is stable at low pH. Lysozyme at 1mg/ml concentration was stressed in an increasing concentration of trifluoroacetic acid (TFA) at 0.1%, 0.5%, and 1.0% for 60 minutes at room temperature. The pH value was less than 2 for all samples. The normalized, overlaid chromatogram in Figure 17 shows that there was no significant change in the degradation peaks and the main peak.

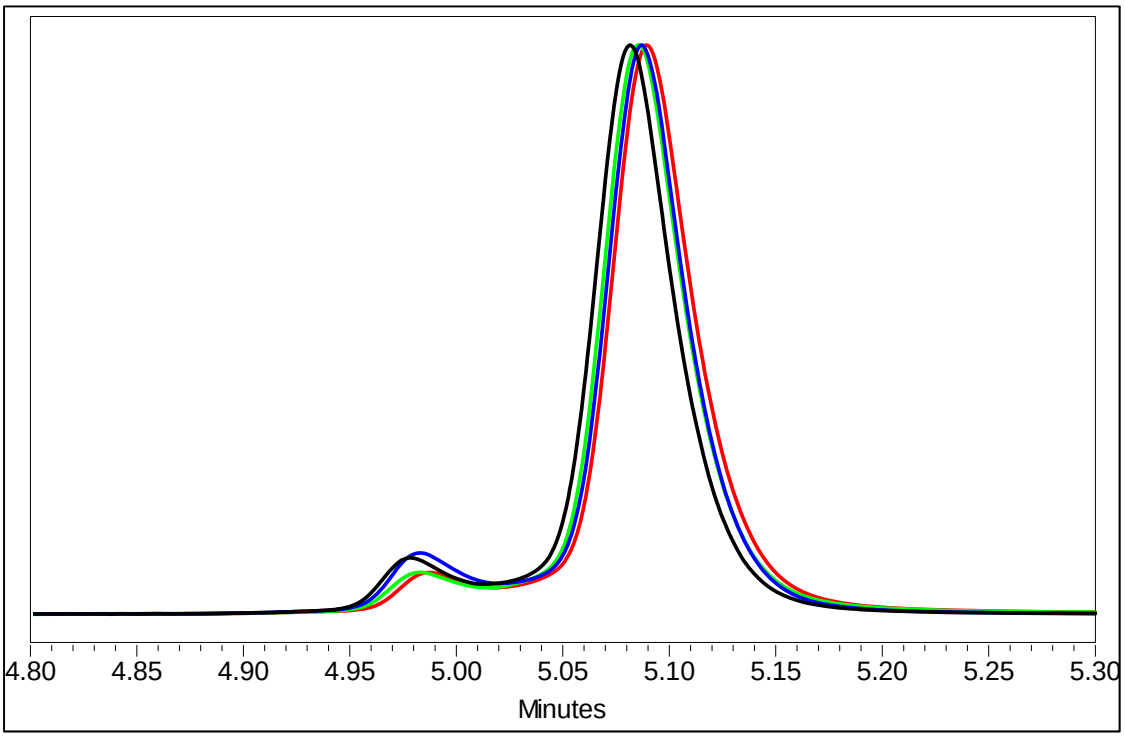

Figure 17 – Normalized, overlaid chromatogram of 1mg/ml lysozyme stressed with trifluoroacetic acid at 0% (Black), 0.1% (Blue), 0.5% (Green), and 1.0% (Red). There was no increase in the degradation peaks observed, and the main peak was unchanged.

Lysozyme Physical Stability

The primary sequence of lysozyme contains 8 cysteines that form 4 intramolecular disulfide bonds. It has been reported in the literature that intramolecular disulfide exchange does occur among these 4 disulfide bonds, forming different conformational isoforms (27,28). Consistent with the findings in the literature, the shifting of conformational isoforms was observed in the current study.

To investigate and show the cause of the conformation shifting, a kinetic study was performed at different solution pH's using the RP-UPLC method for the analysis of lysozyme described in Chapter II. There are 4 noticeable peaks detected using the RP-UPLC method, and these 4 peaks were presumed to be 4 different conformational isoforms of lysozyme. Figure 18 displays the chromatogram of lysozyme using the RP-UPLC method showing the 4 peaks and the relative retention time (RRT) with respects to the main peak. The shifting of the conformational isomers was observed between the main peak and the RRT0.97 peak. Over a period of about 24 hours, the main peak was decreasing (Figure 19) as the RRT0.97 peak was increasing (Figure 20) at the same rate. The rate of conversion is higher at higher pH. The rate constant (k_{obs}) was quantified based on the zero-order reaction, and a pH rate profile was constructed in Figure 21. The conversion between the main peak and the RRT0.97 peak is a reversible process that reaches an equilibrium after 3 hours at pH 8. The conversion rate is very slow at the lower pH's (pH 2.3 and pH 4.5).

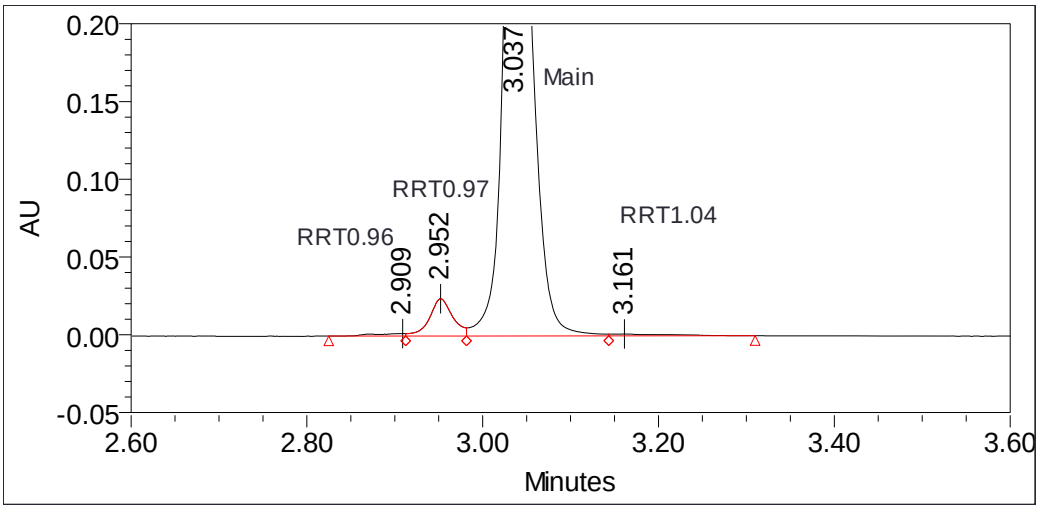

Figure 18 – Representative RP chromatogram of a 1mg/ml lysozyme in 10mM phosphate pH7.4

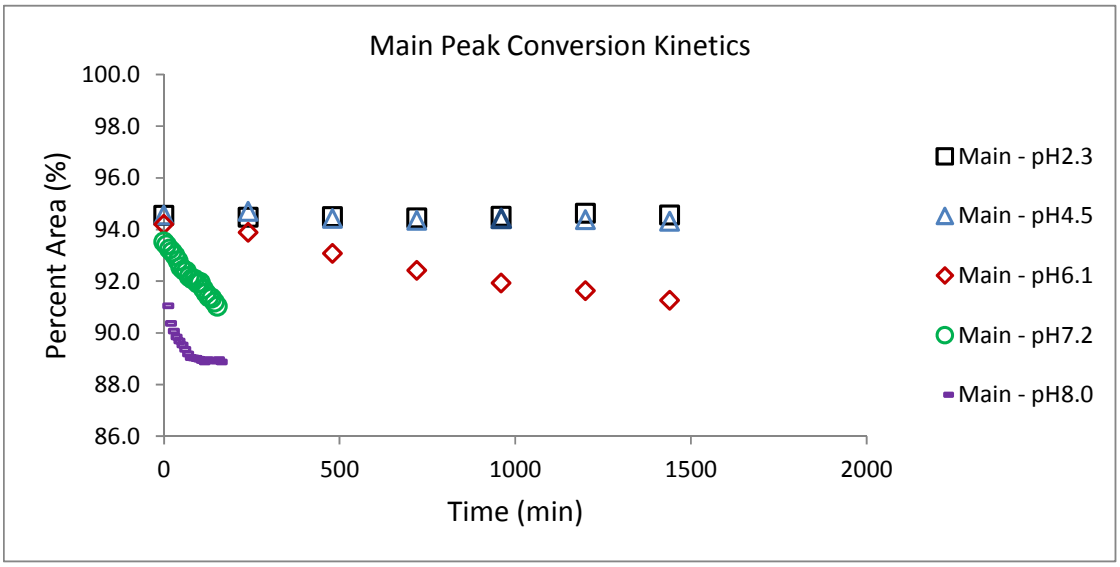

Figure 19 – The kinetics of the decline of the main peak over a period of 24 hours

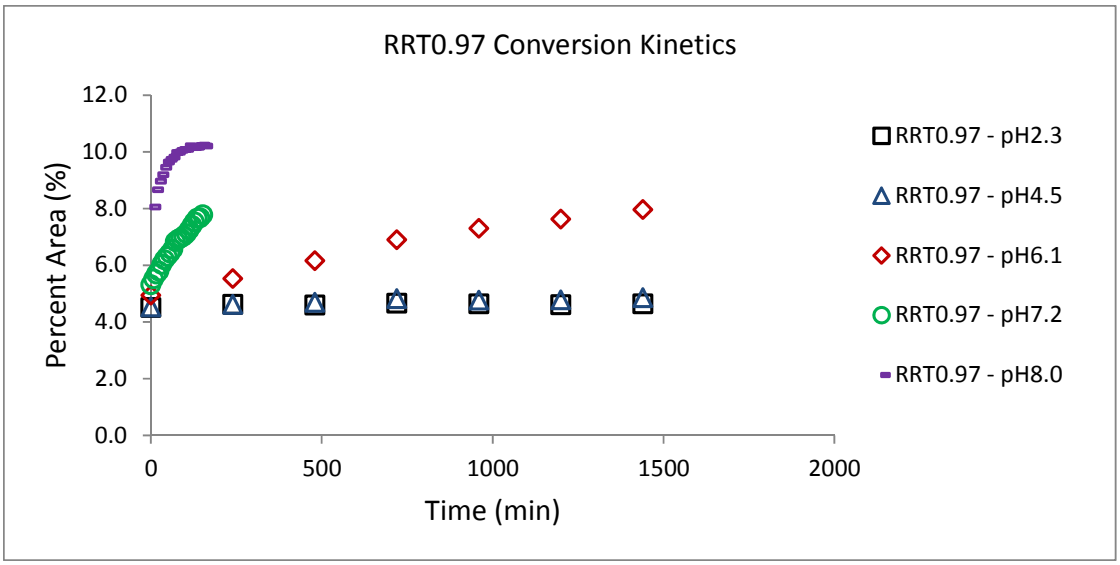

Figure 20 – The kinetics of the increase of peak RRT0.97, which directly mirror the kinetics of the decline of the main peak, indicating that the main peak is converting into peak RRT0.97.

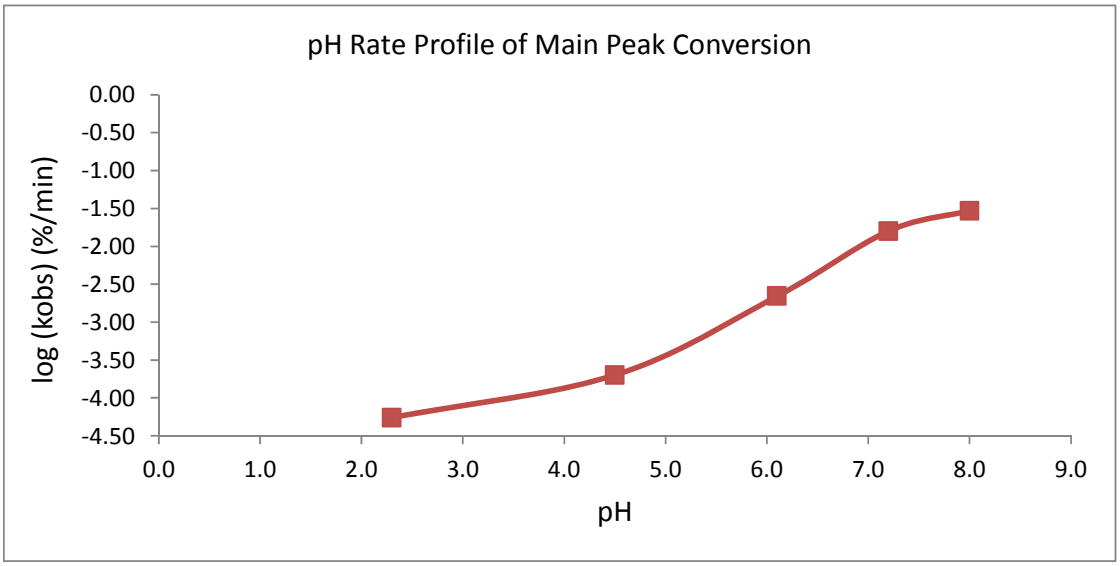

Figure 21 – The pH rate profile of the conversion of the main peak into peak RRT0.97.

The shuffling of the disulfide bonds of lysozyme is a known event, and in Chang and Li 2002, the authors identified the disulfide structures of the native lysozyme and its major scrambled isomers, which are depicted in Figure 22 (29). These species of lysozyme were separated on a RP column with a hydrophobicity ranking in the order of b > N > a > h, which is inversely correlated with the order of elution shown Figure 23. Based on the order of elution/hydrophobicity, it can be reasonably inferred that peak RRT0.97 has the disulfide structure of isomer a, since peak RRT0.97 eluted right before the main/native peak in Figure 18. This order of elution follows the order elution of isomer a and the native in Figure 23. To decisively confirm the identity and disulfide structure of peak RRT0.97, it is necessary to perform mass analysis and Edman sequencing on the isolated species represented as peak RRT0.97 using the methods described in Chang and Li 2002. However, the scope of the current study is to stabilize lysozyme so that the its instability would not interfere with the oxidation stress methods. The pH rate profile in Figure 21 shows that this objective can be achieved if the solution pH is lowered to 3.

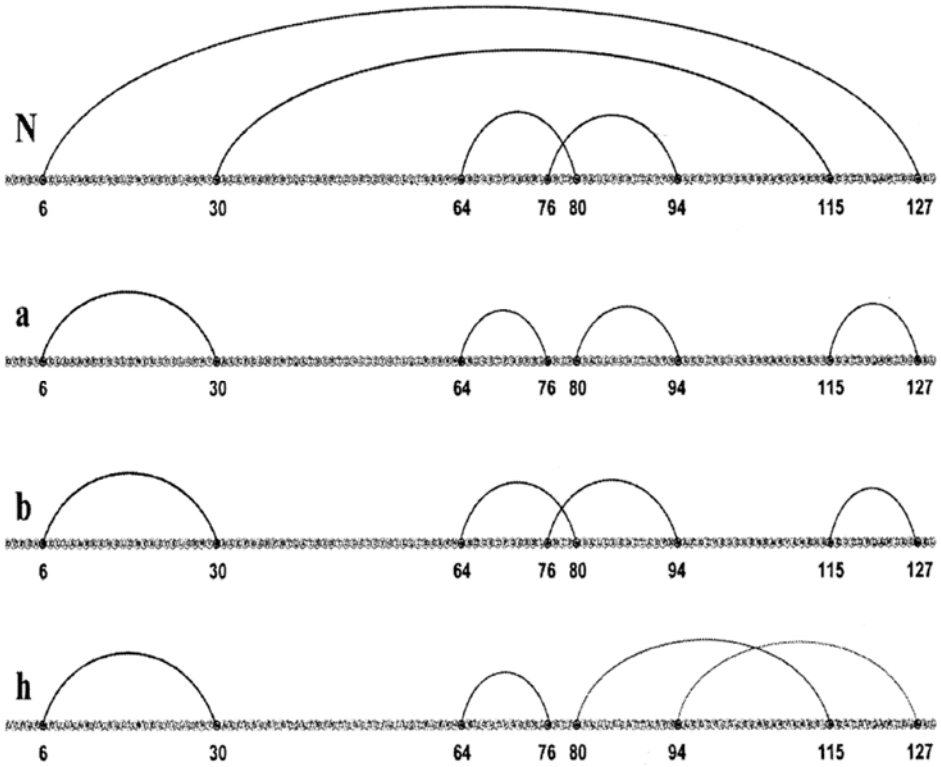

Figure 22 – The disulfide structures of the native lysozyme (N) and three isomers of scrambled lysozyme (a, b and h), reproduced from Chang and Li 2002 with permission.

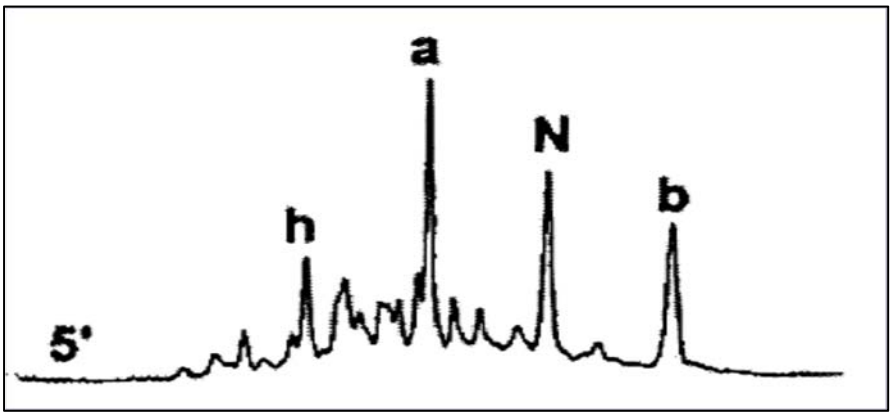

Figure 23 – The separation of the native lysozyme (N) and three isomers of scrambled lysozyme (a, b and h) on a RP column Zorbax 300SB-C18, reproduced from Chang and Li 2002 with permission.

The Degradation of Lysozyme by AAPH

The degradation rate of lysozyme by AAPH is dependent on the concentration of AAPH. Figure 24 shows the steadily decline in the concentration of lysozyme at different concentrations of AAPH. Faster degradation rate of lysozyme was observed in the higher concentration of AAPH. The reaction was allowed to proceed for about 5 - 17 hours at RT in an acidic medium, containing 0.1N HCl with a pH of 3. The analysis was done using the RP-UPLC method described in Chapter II.

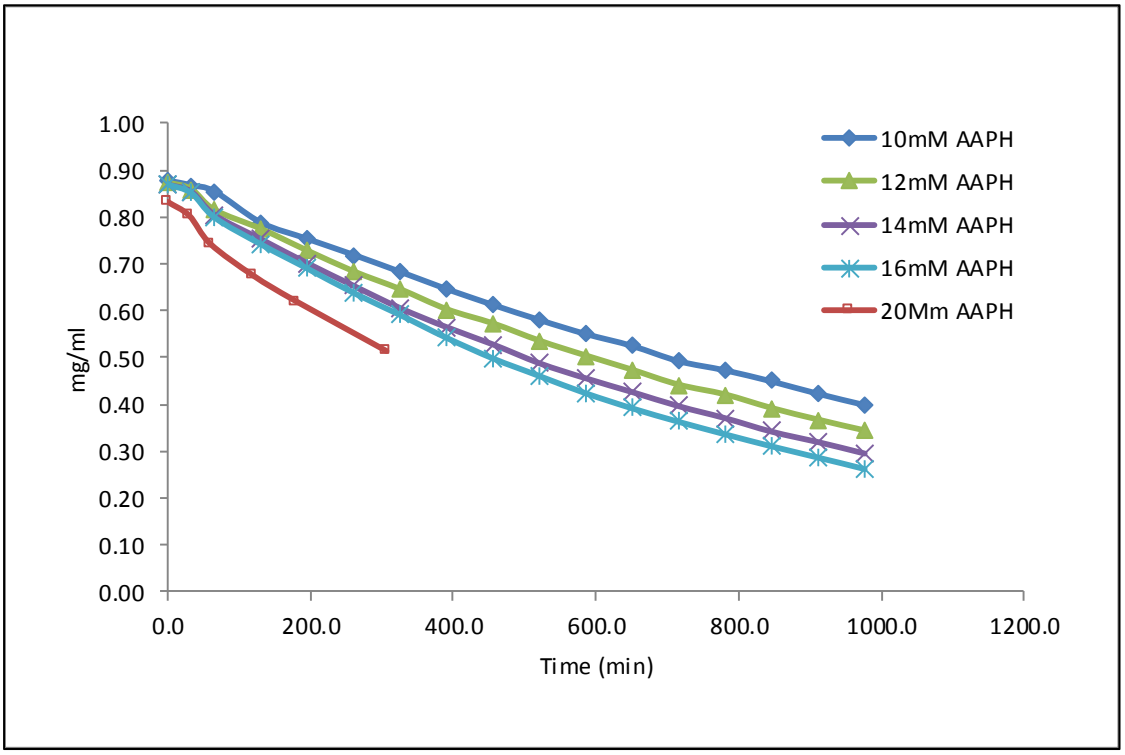

Figure 24 – The declining of lysozyme main peak concentration in the presence of AAPH

The degradation rate seems to follow the first-order kinetics with the correlation coefficient R^2 greater than 0.999 as shown in Figure 25. The first-order rate constants, summarized in Table 6, for the lysozyme degradation rate were determined from the linear plot of ln[concentration] vs time in seconds. Figure 26 shows that there is a linear correlation between the first-order rate constants and the concentration of the AAPH. The direct proportion of the degradation rate (R_d) of lysozyme to the concentration of AAPH leads to Equation 1, where the concentration of AAPH is given in mmol/L (mM) and the first-order rate constant is given in 1/s.

Equation 1: Lysozyme degradation rate (R_d) = 1.31×10^{-6} [AAPH] mM * s^{-1}

The degradation rate of lysozyme by AAPH in this study is about half of the decomposition rate of AAPH determined by Wahl et al. 1998 to be 2.41×10^{-6} [AAPH] mM * s^{-1} (30). While some of the decomposed carbon radicals of AAPH do not escape the solvent cage, the majority of the carbon radicals do diffuse apart and react rapidly with oxygen to form peroxyl radicals (9,30). Therefore, the lower reaction rate of the peroxyl radicals with lysozyme could not be attributed to the trapped carbon radicals.

In addition to the homolytic process of decomposition, AAPH reacts with water to form amide products that do not decompose (30). The authors in Wahl et al. 1998 showed that the first-order rate constant for the formation of the hydrolysis products of AAPH is 2.30×10^{-6} [AAPH] mM * s^{-1}, which is almost equivalent to the decomposition rate of AAPH at 2.41×10^{-6} [AAPH] mM * s^{-1}. This may explain why the reaction rate of the peroxyl radicals with lysozyme is about half of the decomposition rate of AAPH.

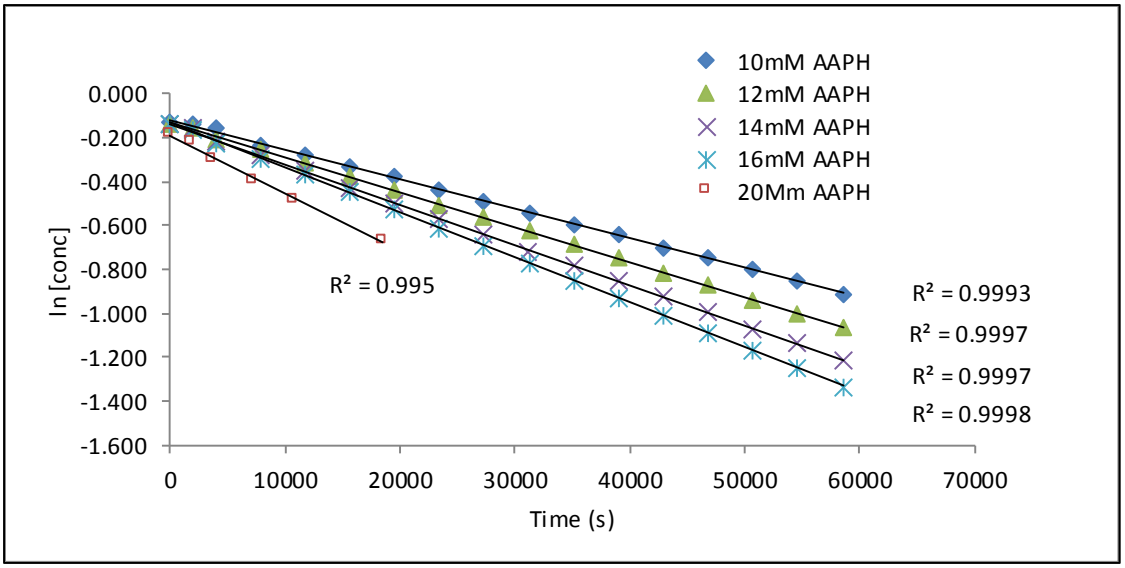

Figure 25 – First-order kinetics of lysozyme degradation by AAPH

Table 6 – First-order rate constants of lysozyme degradation by AAPH

Sample	AAPH Conc (mM)	Rate Constant (1/s)
1mg/ml Lyz in 10mM AAPH, pH3	10	1.34E-05
1mg/ml Lyz in 12mM AAPH, pH3	12	1.59E-05
1mg/ml Lyz in 14mM AAPH, pH3	14	1.84E-05
1mg/ml Lyz in 16mM AAPH, pH3	16	2.04E-05
1mg/ml Lyz in 20mM AAPH, pH3	20	2.64E-05

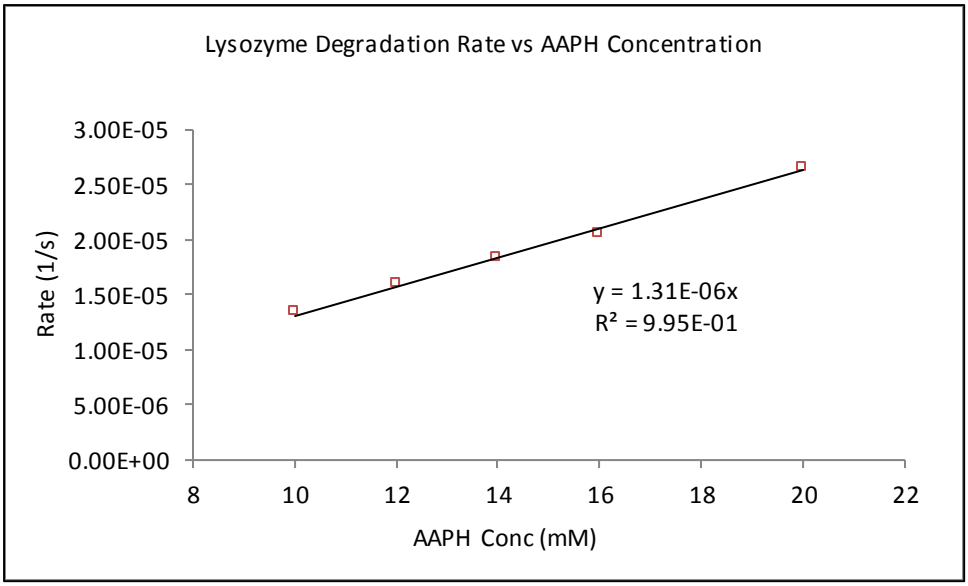

Figure 26 – The degradation rate of lysozyme is linearly correlated to the concentration of AAPH

The main degradation products of lysozyme using AAPH as the oxidant generator are shown in the chromatogram displayed in Figure 27. The formation rates shown in Figure 28 reveal that RRT0.99 is the main degradation product with the fastest zero-order rate of 5.05 x 10^{-6} mg/ml s^{-1} followed by RRT0.96 at 2.95 x 10^{-6} mg/ml s^{-1} and RRT0.97 at 4.64 x 10^{-7} mg/ml s^{-1}. The formation rates of the degradation products of lysozyme using AAPH seem to fit best to zero-order rate kinetics. Fitting the formation rates to the first-order and second-order kinetics showed worse fitting than the zero-order rate kinetics as shown in Figure 29 and Figure 30, respectively.

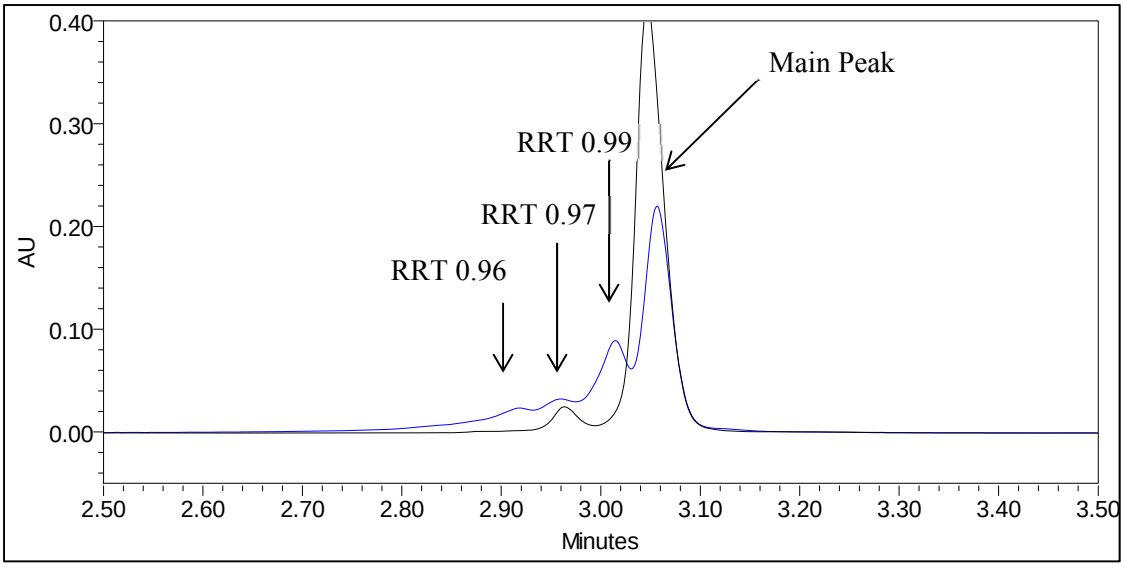

Figure 27 – Formation of lysozyme degradation products after incubation with 16mM AAPH for 480 minutes at room temperature. Black curve represents lysozyme at time = 0. Blue curve represents lysozyme at time = 480 minutes. Main degradation product is peak RRT0.99.

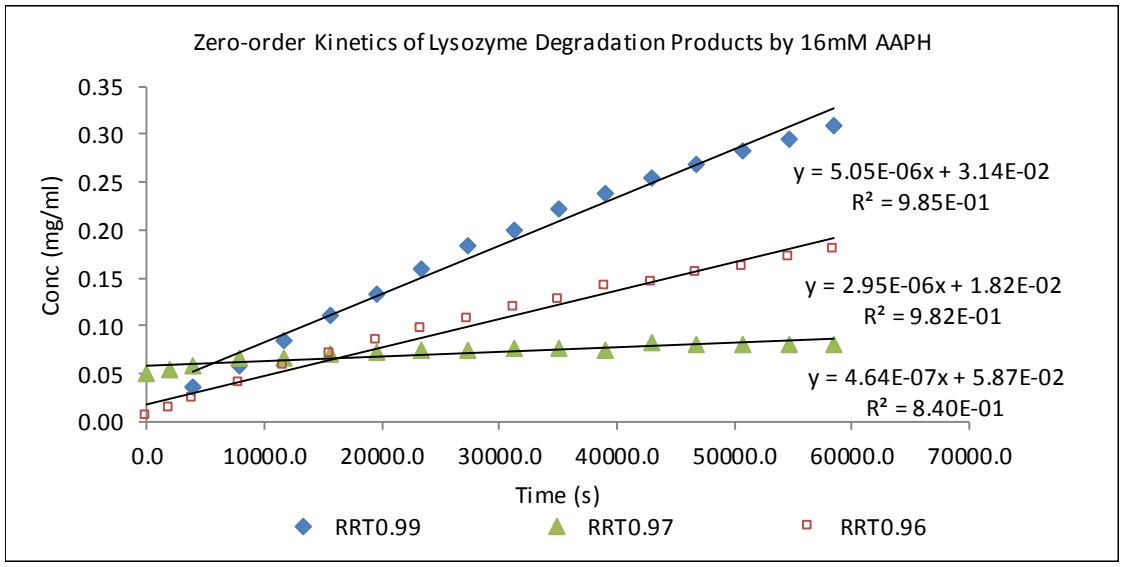

Figure 28 – The formation rates of lysozyme degradation products after incubation with 16mM AAPH for about 17 hours at room temperature seem to follow zero-order kinetics.

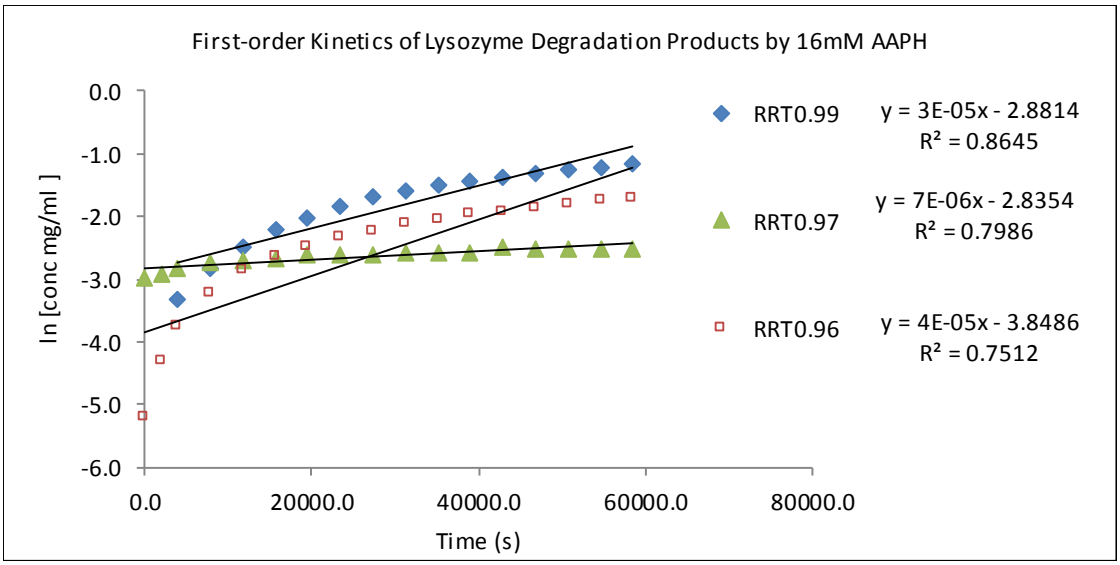

Figure 29 – The kinetics of the degradation products of lysozyme by 16mM AAPH do not seem to fit first-order reaction.

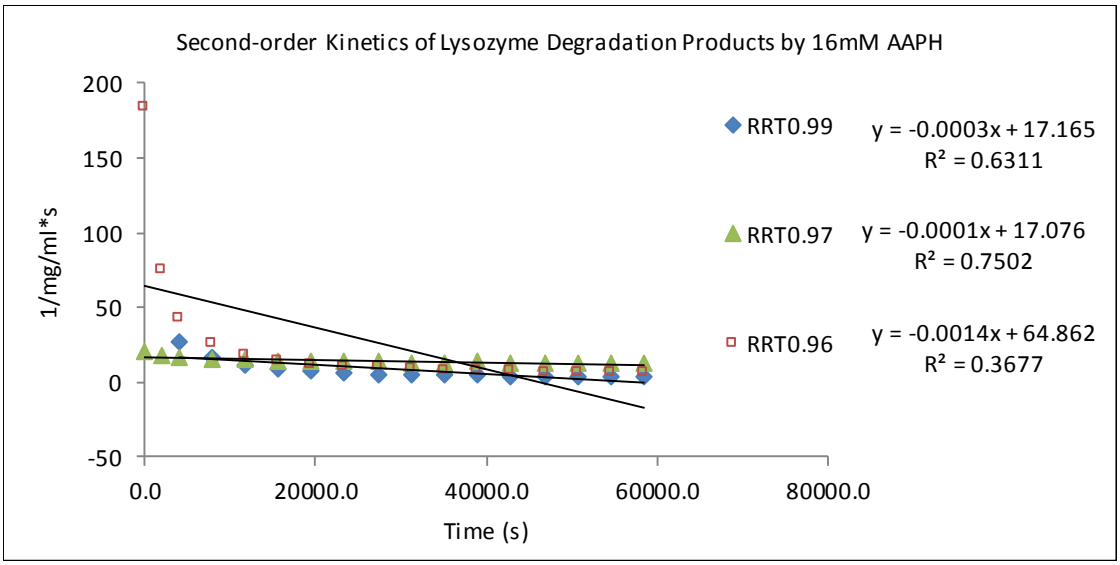

Figure 30 – The kinetics of the degradation products of lysozyme by 16mM AAPH do not seem to fit second-order reaction.

The Degradation of Lysozyme Using the Fenton Reaction

The Fenton reaction is composed of hydrogen peroxide and ferrous ion as a catalyst for the generation of hydroxyl radicals, which are used to induce the oxidation of lysozyme in the current study. The reaction is fast with the rate constant in the range of 40 M^{-1} s^{-1} to 80 M^{-1} s^{-1} depending on the reaction conditions, such as pH, buffer, temperature, etc. (31–33). To perform the kinetics studies for the degradation of lysozyme, a quenching mechanism is required.

Phosphate has been shown to react with the ferrous ion to form ferrous phosphate, an insoluble precipitate (34), and therefore, it has the potential to permanently remove the ferrous ion from the reaction solution, effectively quenching the reaction. The second reagent of the Fenton reaction is hydrogen peroxide, which can oxidize the protein by itself as shown in the Lysozyme Chemical Stability Section. To prevent this potential reaction from occurring, sodium pyruvate was used to react with hydrogen peroxide in a reaction that produces acetic acid and carbon dioxide (35).

To quench the reaction in the current study, 16.4mM of sodium phosphate and 3.3mM sodium pyruvate were added to the Fenton reaction composed of 0.100mM of iron(II) sulfate and 0.544mM of hydrogen peroxide for the oxidation of about 0.07mM of lysozyme. For the Fenton reaction that is composed of lower concentrations of iron(II) sulfate and hydrogen peroxide at 0.040mM and 0.272mM, respectively, about 11.0mM of sodium phosphate and 2.2mM of sodium pyruvate were added to quench the reaction. Figure 31 and Figure 32 show that the concentrations of the quenching reagents chosen for their respective Fenton reactions were effective in quenching the reactions. In both graphs, the degradation of lysozyme proceeded without quenching and but was inhibited after the addition of the quenching reagents.

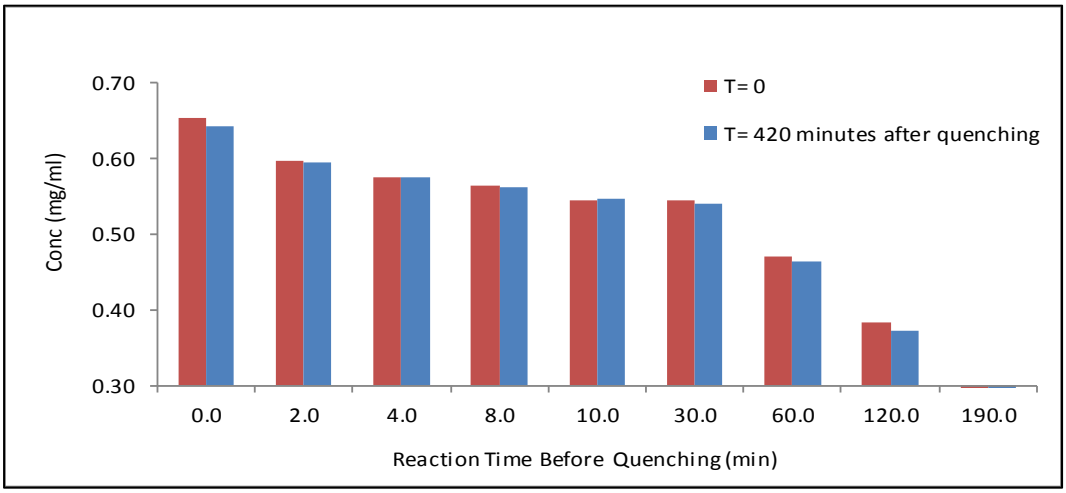

Figure 31 – The Fenton reaction was quenched with the addition of 16.4mM of sodium phosphate and 3.3mM of sodium pyruvate to 0.100mM of iron(II) sulfate and 0.544mM of hydrogen peroxide. The degradation of lysozyme proceeded without quenching as shown in the declining of the lysozyme concentration over a period of 120 minutes. However, there is no significant decline in the lysozyme concentration 420 minutes after the addition of sodium phosphate and sodium pyruvate.

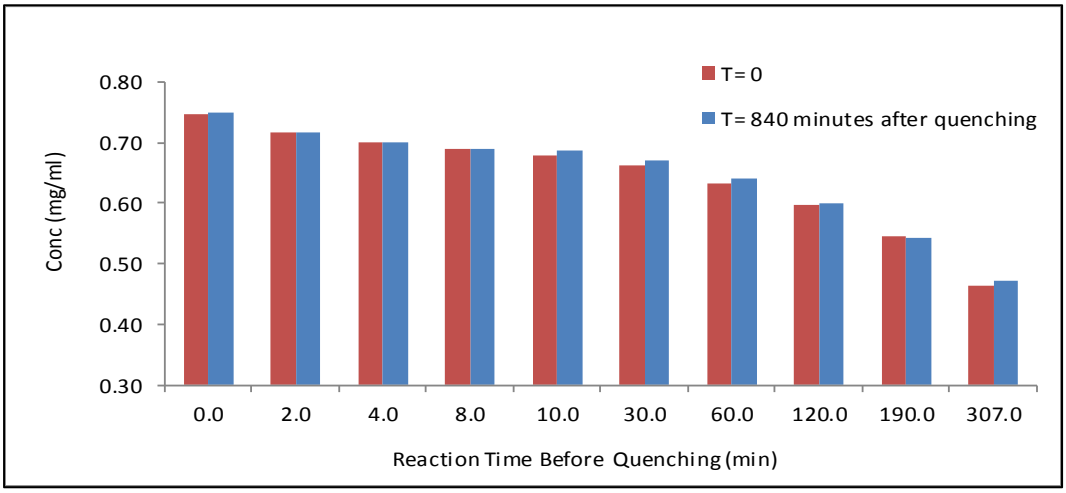

Figure 32 – The Fenton reaction was quenched with the addition of 11.0mM of sodium phosphate and 2.2mM of sodium pyruvate to 0.040mM of iron(II) sulfate and 0.272mM of hydrogen peroxide. The degradation of lysozyme proceeded without quenching as shown in the declining of the lysozyme concentration over a period of 307 minutes. However, there is no significant decline in the lysozyme concentration 840 minutes after the addition of sodium phosphate and sodium pyruvate.

The degradation of lysozyme was observed using the RP-UPLC analysis. The declining of lysozyme main peak in the presence of the Fenton reagents is shown in Figure 33. Consistent with the findings in Rachmilovich-Calis et al. 2009, the observed degradation kinetics do not seem to fit a single exponential rate law when excess hydrogen peroxide was used (32). The data were then fitted to a double exponential function based on first-order kinetics for the fast reaction (Figure 34) and the slow reaction (Figure 35). The first-order rate constants for the fast reaction and slow reaction are summarized in Table 7.

Although fitted to a double exponential function, the correlation does not seem to fit well for the fast reaction in Figure 34. The cause for this non-linear correlation could be attributed to the fact that the addition rate of the quenching reagents and the subsequent quenching reaction rate could be much slower than the degradation rate of lysozyme by the Fenton reaction.

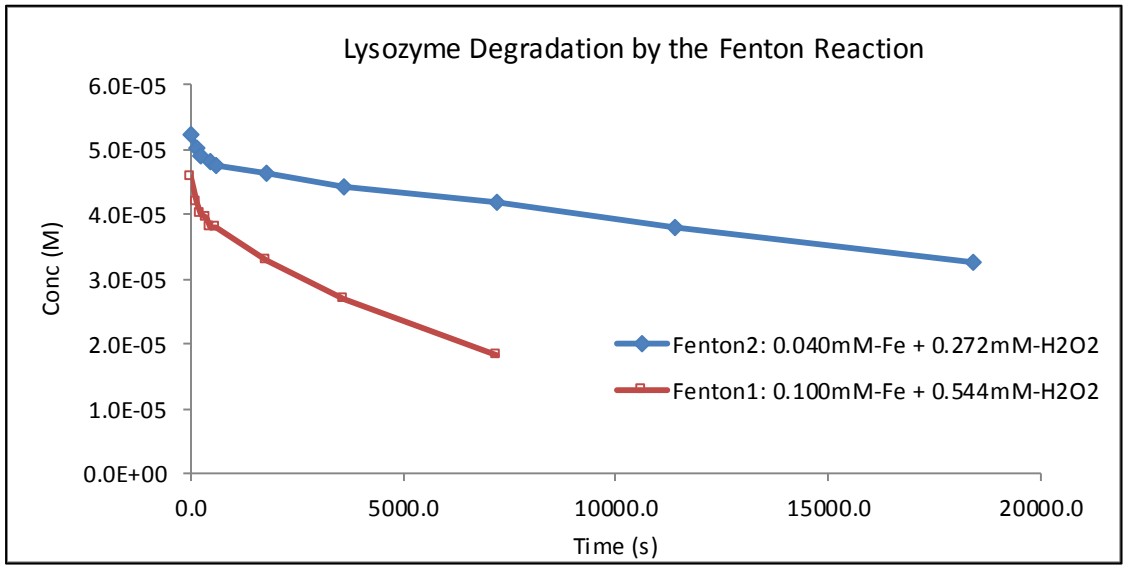

Figure 33 – The declining of lysozyme main peak concentration in the presence of iron(II) sulfate and hydrogen peroxide at different concentrations.

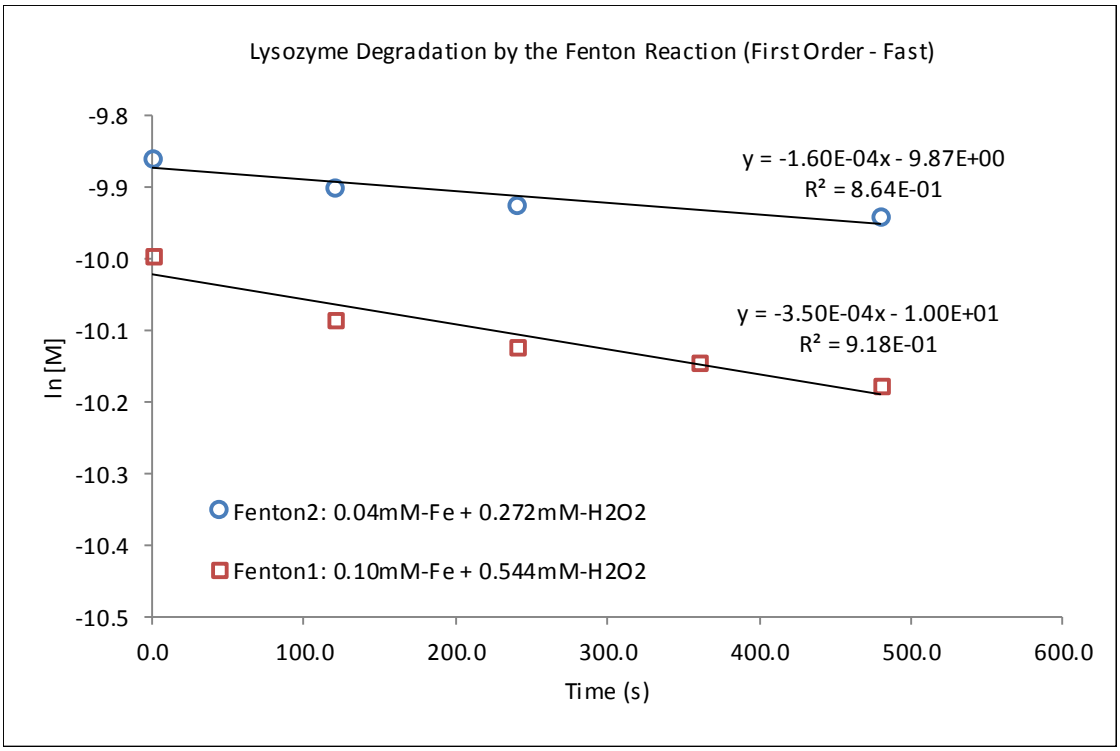

Figure 34 – First-order kinetics of the degradation of lysozyme by the Fenton reaction (Fast).

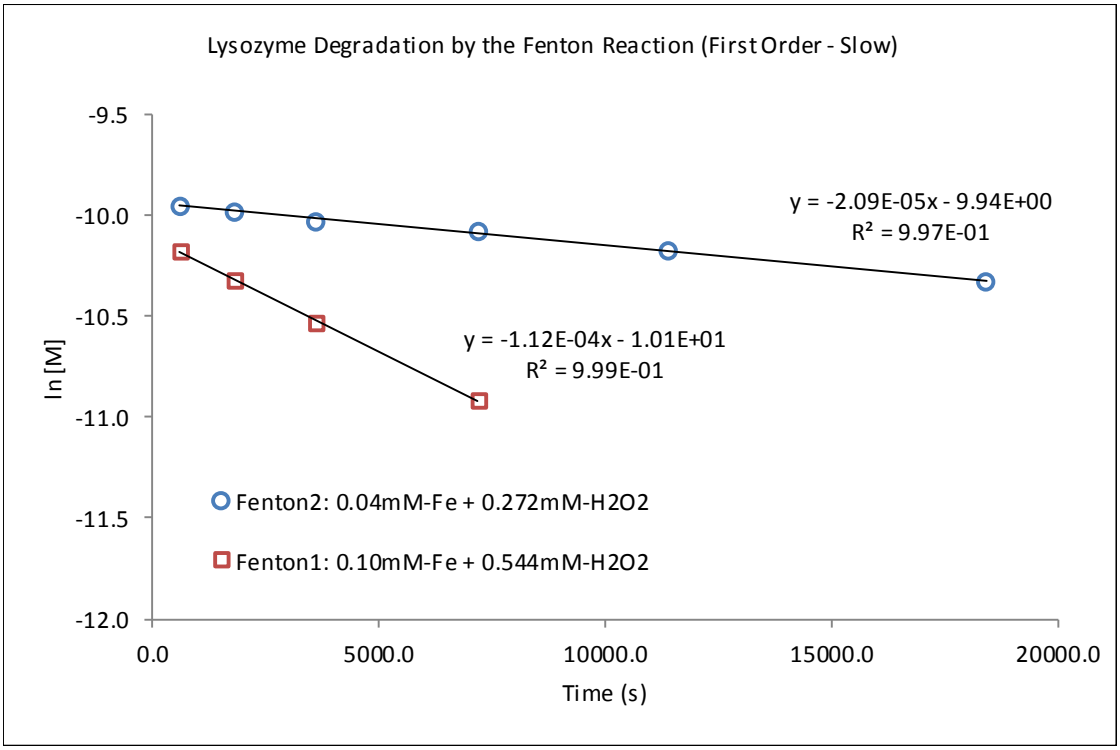

Figure 35 – First-order kinetics of the degradation of lysozyme by the Fenton reaction (Slow).

Table 7 – First-order rate constants of lysozyme degradation by the Fenton reaction

Sample	$FeSO_4$ (mM)	H_2O_2 (mM)	Fast Rate Constant (1/s)	Slow Rate Constant (1/s)
0.07mM Lyz in 0.040mM $FeSO_4$ + 0.272mM H_2O_2	0.040	0.272	1.60×10^{-4}	2.09×10^{-5}
0.07mM Lyz in 0.100mM $FeSO_4$ + 0.544mM H_2O_2	0.100	0.544	3.50×10^{-4}	1.12×10^{-4}

The main degradation products of lysozyme using the Fenton reaction are shown in the chromatogram displayed in Figure 36. There was an increase in all the related species of lysozyme as the main peak decreases. The kinetics curves of formation rate of the degradation products are displayed in Figure 37. The kinetics do not seem to fit any rate law, but the formation rate of peak RRT0.94 seems to be the fastest.

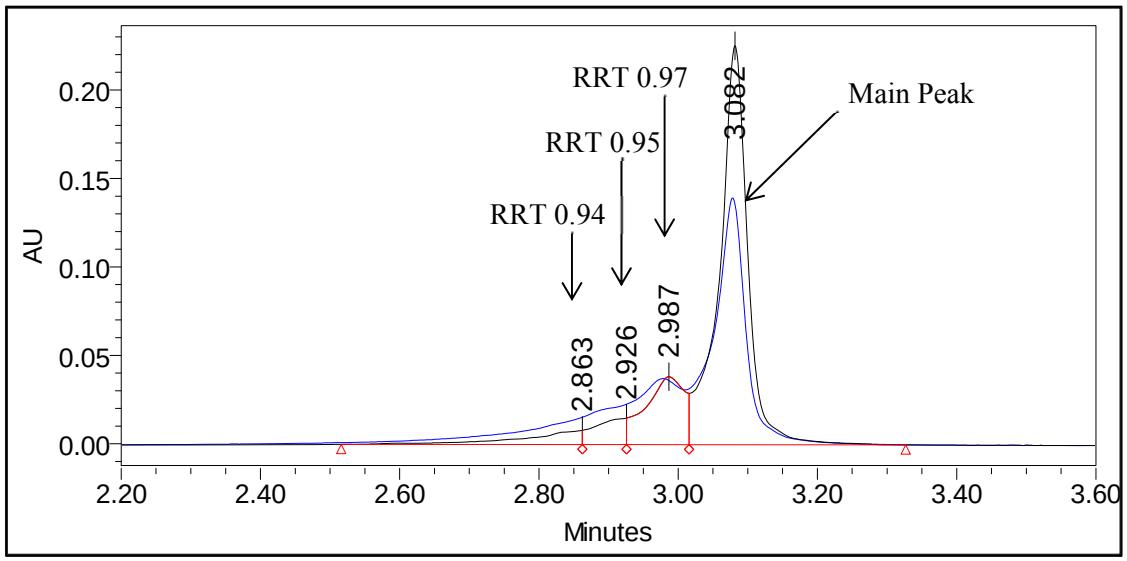

Figure 36 – Overlaid chromatogram of lysozyme degradation products after incubation with the Fenton reaction reagents (0.100mM $FeSO_4$ + 0.544mM H_2O_2), 30 minutes at room temperature. Black curve represents lysozyme at time = 0. Blue curve represents lysozyme at time = 30 minutes.

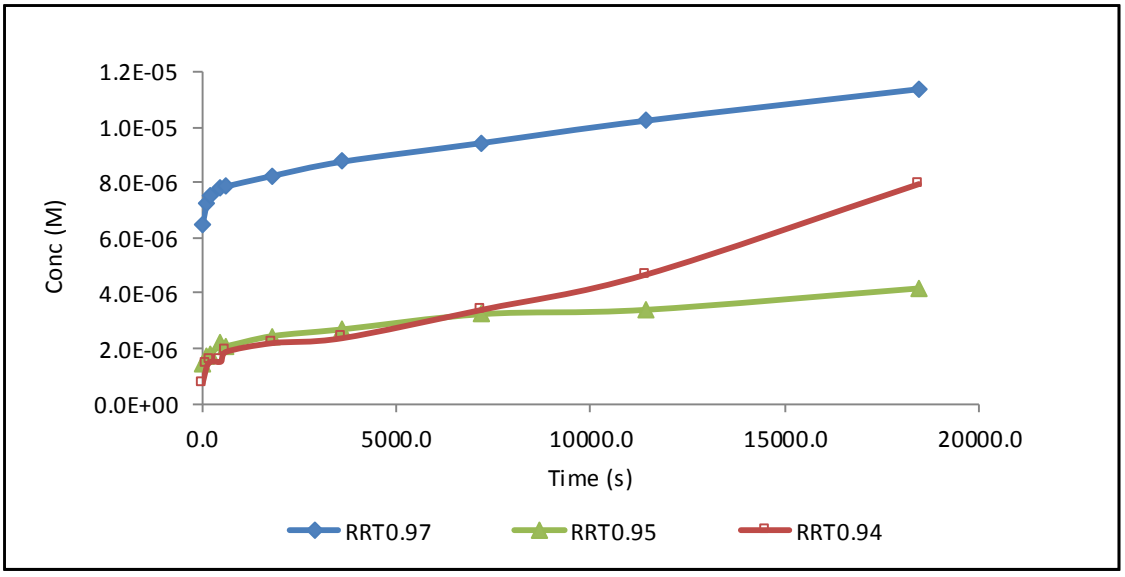

Figure 37 – Kinetics of lysozyme degradation products by the Fenton reaction. The rate of formation seems to be fastest for peak RRT0.94.

Lysozyme Degradation by Ionizing Radiation, AAPH, and the Fenton reaction

The degradation of lysozyme by ionizing radiation was studied using gamma rays from a ^{60}CO source. Lysozyme solid powder was prepared and irradiated as described in Chapter II. The irradiated samples were then dissolved in 0.1N HCl and analyzed by the RP-UPLC method, the SEC method, and the tryptophan analysis method described in Chapter II. The pH of the sample was around 3, the ideal pH for lysozyme's physical stability. For control, non-irradiated lysozyme samples were dissolved in the same diluent and analyzed concurrently with the irradiated samples. All samples were prepared in triplicates.

The results from the RP-UPLC analysis indicate that the irradiation process affects about 7% of the native species of lysozyme as seen in the decrease of the peak area percent of the main peak from 94.2% to 86.4%. Peak RRT1.04 is the prominent degradation product of the irradiation process. The peak area percent of RRT1.04 from the gamma-irradiated lysozyme is 6.5%

compared to a 0.5% peak area percent from the control. Other peaks with noticeable peak area percent increase are peak RRT0.94 and peak RRT0.95. The results of the RP-UPLC analysis of the gamma-irradiated lysozyme are outlined in Table 8. The labeling of the peaks is displayed in the overlaid chromatogram in Figure 38. Since peak RRT1.04 elutes later than the main peak, it is presumed that this group of species is more hydrophobic than the native species of lysozyme.

Table 8 – The results of the RP-UPLC analysis of the gamma-irradiated lysozyme

Sample	RP-UPLC Peak Area (%), (average ± deviation, n=3)				
	Main Peak	RRT0.94	RRT0.96	RRT0.97	RRT1.04
Control, Native Lysozyme	94.2 ± 0.1	0.2 ± 0.0	0.2 ± 0.0	4.8 ± 0.0	0.5 ± 0.1
Gamma-Irradiated Lysozyme	86.4 ± 0.4	0.6 ± 0.0	0.4 ± 0.1	6.1 ± 0.1	6.5 ± 0.3

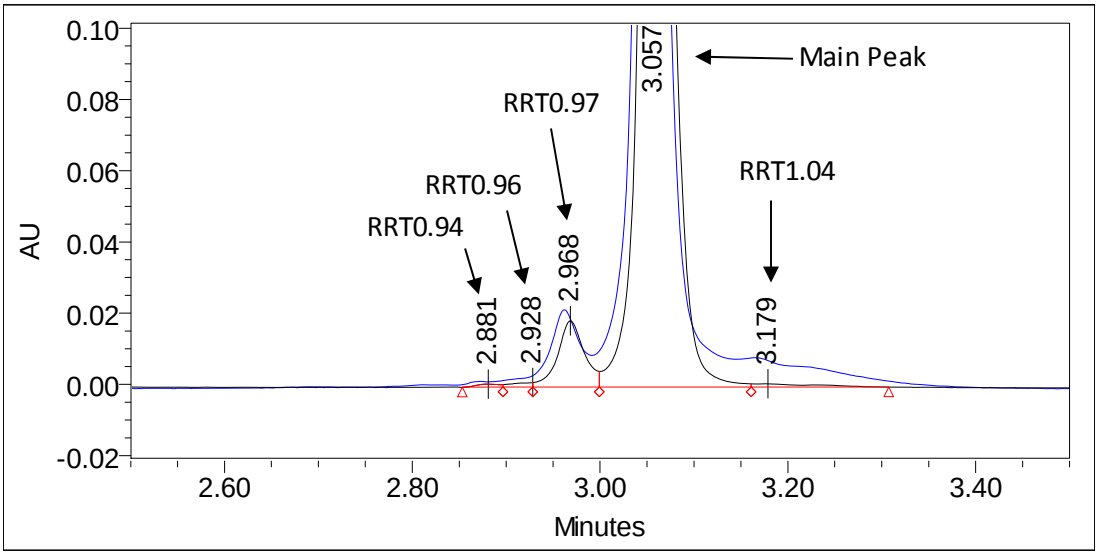

Figure 38 – Overlaid RP-UPLC chromatogram of gamma-irradiated lysozyme (blue curve) with the non-irradiated lysozyme (black curve). Peak RRT1.04 is the most prominent degradation product resulted from the irradiation process.

The results from the SEC analysis show that the aggregation of lysozyme increases after the irradiation process. The intended objective of the SEC method is to assess the effect of protein aggregation. Aggregated proteins, referred to as HMW species, have larger hydrodynamic size than the monomeric form and therefore, elute earlier. Peak RRT0.93, eluting earlier than the main peak and thereby, representing the HMW species of lysozyme, is about 6.5% higher in the gamma-irradiated lysozyme than in the non-irradiated lysozyme. The results of the SEC analysis of the gamma-irradiated lysozyme are outlined in Table 9. The labeling of the peaks is displayed in the overlaid SEC chromatogram in Figure 39.

Table 9 – The results of the SEC analysis of the gamma-irradiated lysozyme

Sample	SEC Peak Area (%), Average, n=3			
	Monomer	Std. Dev.	RRT0.93	Std. Dev.
Control, Native Lysozyme	99.2	0.0	0.8	0.0
Gamma-irradiated Lysozyme	92.7	0.2	7.3	0.2

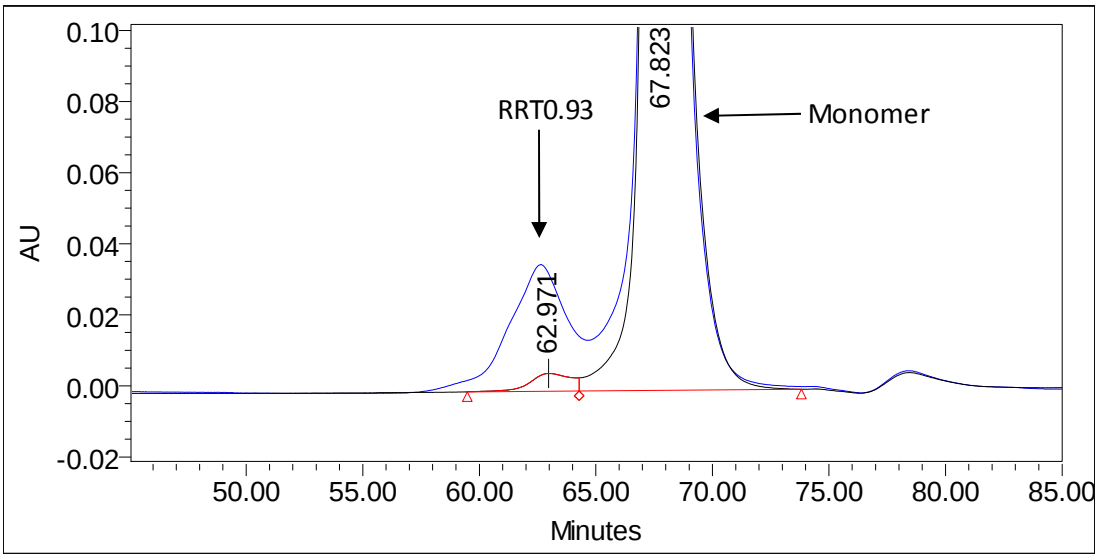

Figure 39 – Overlaid SEC chromatogram of gamma-irradiated lysozyme (blue curve) with the non-irradiated lysozyme (black curve). Peak RRT0.93 is the most prominent degradation product resulted from the irradiation process.

The SEC results align with the results from the RP-UPLC analysis. The RP-UPLC analysis shows that the irradiation process generated about 6.0% of the degradants that are more hydrophobic than the native species. In the SEC analysis, about 6.5% of the native species aggregated into HMW species because of the irradiation process. In general principles, the aggregated form of the protein is more hydrophobic than the monomeric form when the analysis is done using reversed phase liquid chromatography since the aggregated form has more carbon bonds than the monomeric form.

To assess the effect of ionizing radiation on the tryptophan residue on the protein, gamma-irradiated and non-irradiated lysozyme samples were hydrolyzed using the tryptophan analysis method in Chapter II. The hydrolyzed samples were then analyzed by the RP-UPLC method listed in Table 3. The data in Table 10 show that although there was about 7% of the tryptophan residues affected by the irradiation process, the difference between the irradiation group and the control group was not statistically significant with a p-value of 0.119. The p-value was derived using the Student's paired T-test with 2 tails distribution. Figure 40 displays the tryptophan recoveries of the 2 groups in a high-low graph.

Table 10 – The results of the Tryptophan Analysis of the gamma-irradiated lysozyme

Sample	Prep	Trp Recovery (%)	Average (%)	Std Dev (%)	%Damage	P-Value
Control, Native Lysozyme	1	93.1	94.8	1.9	n/a	n/a
	2	94.5				
	3	96.7				
Gamma-irradiated Lysozyme	1	89.0	88.3	2.6	6.8	0.119
	2	90.5				
	3	85.4				

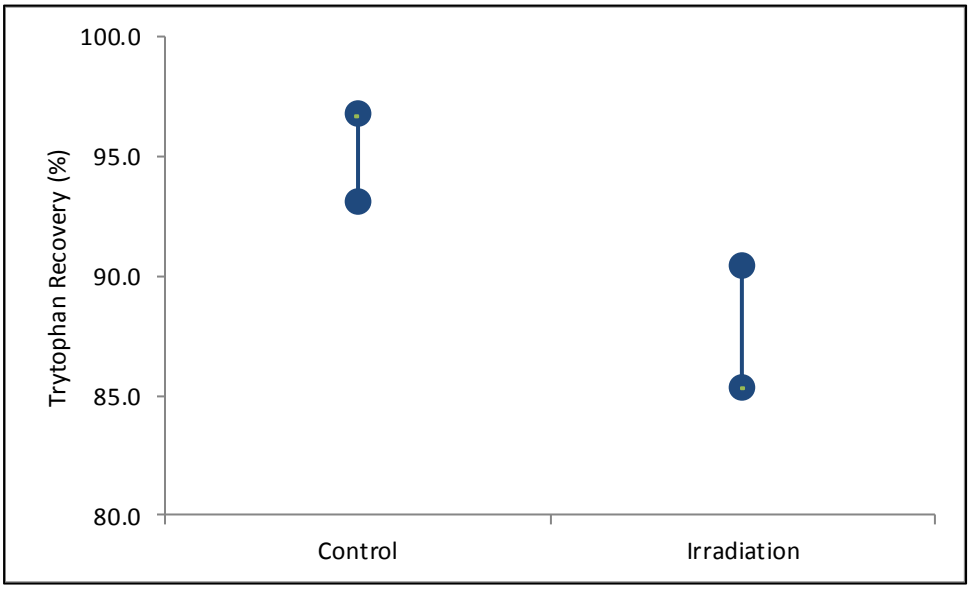

Figure 40 – The percent recovery of tryptophan from the control group (non-irradiated) and the gamma-irradiated group. The difference was not statistically significant at $p = 0.119$

The results of the analyses of irradiated and non-irradiated lysozyme indicate that the irradiation process affects lysozyme mainly by inducing aggregation while other degradation pathways play a smaller role. To simulate the effect of the irradiation process, the surrogate forced degradation methods should show similar results to be valid as a screening tool for stabilizing agents against ionizing radiation. Also, the degradation of the protein can be resulted in multiple parallel pathways depending on the forced degradation method and the degree of the degradation (11).

To aptly compare the forced oxidation methods, such as the Fenton reaction and the azo initiator AAPH, to the effect of ionizing radiation on the model protein lysozyme, it is of significance to deliberately degrade the protein to the equivalent degree across all processes.

The degradation rates of lysozyme were determined for both the azo initiator AAPH and Fenton reaction, and the degree to which the ionizing radiation effect lysozyme is about 7% according to the RP-UPLC analysis. To degrade about 7% of lysozyme using 20mM AAPH and the Fenton reaction comprising of 0.040mM of iron(II) sulfate and 0.272mM of hydrogen peroxide, the durations required for the stress degradation period at room temperature are 46 minutes for 20mM AAPH and about 50 minutes for the Fenton reaction after taking into account of both the fast reaction and the slow reaction. The calculations of the derived forced degradation periods are shown in Table 11.

Table 11 – The calculation of the required duration for the forced degradation methods.

Oxidative Agent	Initial Conc $[A]_0$	Target Conc [A]	Rate Constant (k)	Reaction Order	Integrated Rate Law	Time (t), min
20mM AAPH	100	93	2.64E-05 s^{-1}	First	$[A] = [A]_0e^{-kt}$	46
Fenton Reaction, Fast	100	93	1.60E-04 s^{-1}	First	$[A] = [A]_0e^{-kt}$	8
Fenton Reaction, Slow	100	93	2.09E-05 s^{-1}	First	$[A] = [A]_0e^{-kt}$	58

Forced degradation by 20mM AAPH was performed in triplicates at a protein concentration of 1mg/ml in 0.1N HCl. The samples were incubated at room temperature with mixing for a total of 46 minutes. Concurrently, 3 vials of 1mg/ml of lysozyme in 0.1N HCl were incubated in 0.040mM of iron(II) sulfate and 0.272mM of hydrogen peroxide to perform the forced

degradation by the Fenton reaction. These Fenton-stressed samples were incubated at room temperature with mixing for a total of 47 minutes.

The data in Table 12 show that per RP-UPLC analysis, the main peak of lysozyme was degraded similarly across all three oxidation methods at about 84.8% to 87.6%. However, the degradation products were different for all three methods. The main degradation product resulting from the gamma irradiation process is RRT1.04. Both 20mM AAPH and the Fenton reaction methods did not affect the peak area percent of peak RRT1.04 significantly or to the degree that was observed in the gamma irradiation process. The main degradation product for the 20mM AAPH is RRT0.99, which was not detected in the gamma-irradiated sample, the Fenton-stressed sample, and the control. RRT0.97 is the predominant degradation product resulted from the Fenton reaction. Figure 41 displays the RP-UPLC overlaid chromatograms showing various degradation products. The results from the RP-UPLC method indicate that all three oxidation methods seem to degrade lysozyme differently.

Table 12 – The comparison of the RP-UPLC results across different oxidation methods

Sample	RP-UPLC Peak Area (%), n=3						Recovery (%)
	Main Peak	RRT0.94	RRT0.96	RRT0.97	RRT0.99	RRT1.04	
Control, Native Lysozyme	94.2	0.2	0.2	4.8	n/a	0.5	91.5
Gamma-Irradiated Lysozyme	86.4	0.6	0.4	6.1	n/a	6.5	90.5
20mM-AAPH-stressed Lysozyme	84.8	0.7	1.0	6.4	6.6	0.6	93.3
Fenton-stressed Lysozyme	87.6	1.8	1.0	8.8	n/a	0.8	91.6

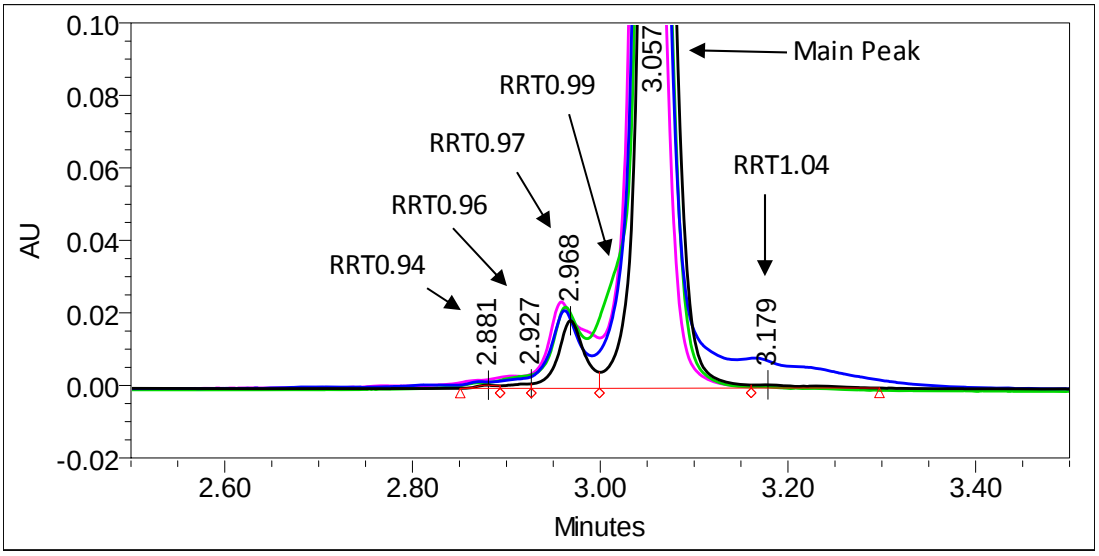

Figure 41 – Overlaid chromatogram of the RP-UPLC analysis of the control (Black), gamma-irradiated (Blue), 20mM AAPH stressed (Green), and the Fenton reaction stressed sample (Pink).

The data in Table 13 show that per SEC analysis, the 20mM-AAPH-stressed lysozyme and the Fenton-stressed lysozyme do not have as high number of aggregated species as the gamma irradiation process. The aggregated species of lysozyme, represented by peak RRT0.93, increased from 0.8% in the control to 1.6% in the 20mM-AAPH-stressed lysozyme and to 3.6% in the Fenton-stressed lysozyme, whereas the gamma irradiation process generated as much as 7.3% of the aggregated species. The results from the SEC analysis are consistent with the results from the RP-UPLC in showing that the simulated degradation methods did not generate the same amount of degradants as the actual irradiation process.

Table 13 – The comparison of the SEC results across different oxidation methods

Sample	SEC Peak Area (%), Average, n=3				Recovery (%)	Std. Dev.
	Monomer	Std. Dev.	RRT0.93	Std. Dev.		
Control, Native Lysozyme	99.2	0.0	0.8	0.0	91.9	1.6
Gamma-irradiated Lysozyme	92.7	0.2	7.3	0.2	86.2	1.2
20mM-AAPH-stressed Lysozyme	98.4	0.1	1.6	0.1	93.1	1.4
Fenton-stressed Lysozyme	96.4	0.7	3.6	0.7	92.8	0.8

The data in Table 14 show that the amino acid residue tryptophan was affected significantly by the 20mM AAPH method and the Fenton reaction method. About 25.0% of the tryptophan was damaged by the 20mM AAPH method, and 18.3% of the tryptophan was damaged by the Fenton reaction with respect to the control. The differences were statistically significant with the p-value at 0.036 for the 20mM AAPH and 0.012 for the Fenton reaction. The p-values were derived using the Student's paired T-test with 2 tails distribution. In contrast with the forced degradation methods, the gamma irradiation process affected only about 6.8% of the tryptophan residue with respect to the control, and the difference was not statistically significant with the p-value at 0.119. For statistically significant differences, the p-value should be at or below 0.05. Figure 42 displays the data in Table 14 in a high-low graph.

Table 14 – The comparison of the tryptophan recoveries across different oxidation methods

Sample	Prep	Trp Recovery (%)	Average (%)	Std Dev (%)	%Damage	P Value
Control, Native Lysozyme	1	93.1	94.8	1.9	n/a	n/a
	2	94.5				
	3	96.7				
Gamma-irradiated Lysozyme	1	89.0	88.3	2.6	6.8	0.119
	2	90.5				
	3	85.4				
20mM-AAPH-stressed Lysozyme	1	70.9	71.0	6.7	25.0	0.036
	2	77.8				
	3	64.4				
Fenton-stressed Lysozyme	1	72.5	77.4	5.2	18.3	0.012
	2	76.8				
	3	82.8				

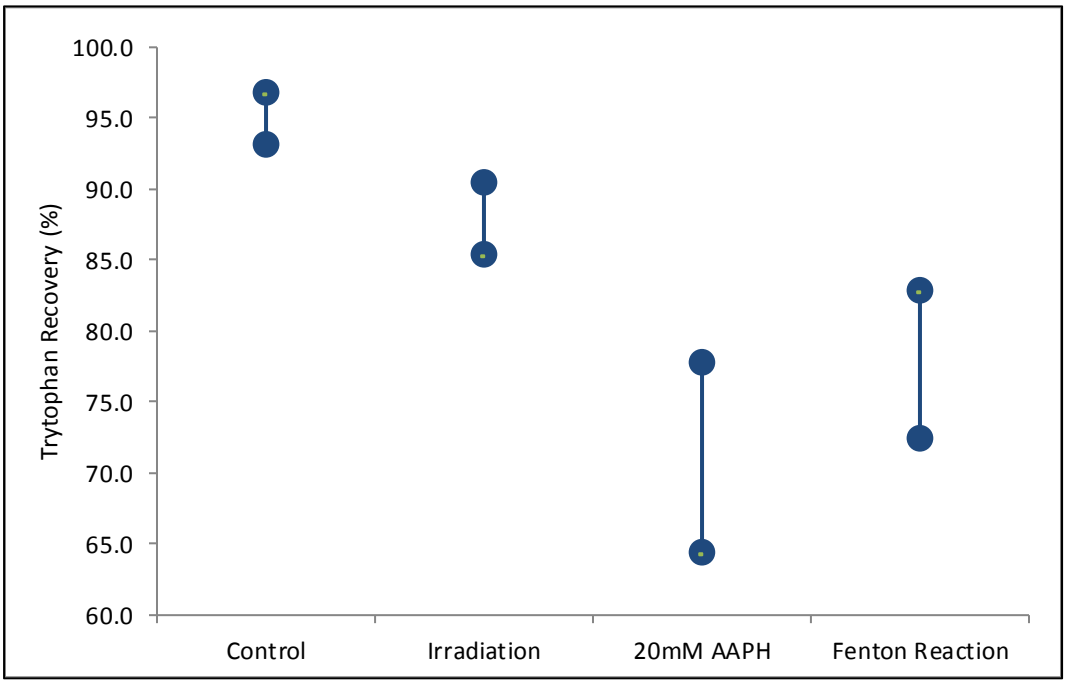

Figure 42 – High-low graph of the recovery of tryptophan from degraded lysozyme using gamma irradiation, 20mM AAPH, and the Fenton reaction.

CHAPTER IV: CONCLUSION

The current study was designed to address the validity of the use of oxidants generators, such as AAPH and the Fenton reaction, as a screening tool to identify stabilizing agents against ionizing radiation for biopharmaceutical products. Lysozyme was chosen as the model protein, and the degradation kinetics was evaluated using AAPH and the Fenton reaction. The results show that both oxidation stress methods are effective in degrading lysozyme. However, the mechanism is seemingly different between the two methods due to the observation of different degradation products and reaction rates. This is expected since the oxidants derived from these oxidation methods are different. While AAPH generates peroxyl radicals, the Fenton reaction produces hydroxyl radicals.

Comparably, the gamma irradiation process also generates radicals that can potentially oxidize proteins in the same way as the radicals derived from the azo compound AAPH and the Fenton reaction do. However, in addition to oxidation, gamma irradiation also has other damaging effects on the proteins that the oxidation methods may not be able to replicate individually. The current research shows that in addition to oxidation, lysozyme is also prone to aggregation when exposed to gamma rays in solid state and that the aggregation effect is more prominent than the oxidation effect. While both AAPH and the Fenton reaction can oxidize lysozyme effectively, the methods were not able to reproduce the aggregation effect for lysozyme at the same level as the irradiation process. Therefore, the use of these methods as a screening tool for stabilizing agents may not be effective.

Limitations

The scope of this study was to compare the degradation pattern of lysozyme subjected to gamma irradiation, AAPH, and the Fenton reaction, and therefore, the identification of the unknown degradants was not done in a comprehensive way. Further research may be warranted to prove the true identity of the unknown degradants in this study, such as the peaks observed in the RP-UPLC method, especially peak RRT0.97.

REFERENCES

1. Center for Drug Evaluation and Research (CDER), Center for Veterinary Medicine (CVM). Guidance for Industry for the Submission Documentation for Sterilization Process Validation in Applications for Human and Veterinary Drug Products. Silver Spring, MD: Food and Drug Administration (FDA); 1994.
2. Headlam HA, Davies MJ. Beta-scission of side-chain alkoxyl radicals on peptides and proteins results in the loss of side-chains as aldehydes and ketones. Free Radic Biol Med. 2002;32(11):1171–1184.
3. Kempner ES, Whittaker JW, Miller JH. Radiation inactivation of galactose oxidase, a monomeric enzyme with a stable free radical. Protein Sci. 2010 Feb;19(2):236–41.
4. Terryn H, Deridder V, Sicard-Roselli C, Tilquin B, Houée-Levin C. Radiolysis of proteins in the solid state: an approach by EPR and product analysis. J Synchrotron Radiat. 2005 May 1;12(3):292–8.
5. Lee Y, Song KB. Effect of gamma-irradiation on the molecular properties of myoglobin. J Biochem Mol Biol. 2002;35(6):590–594.
6. Edwards AM, Ruiz M, Silva E, Lissi E. Lysozyme Modification by the Fenton Reaction and Gamma Radiation. Free Radic Res. 2002 Jan;36(3):277–84.
7. Sellak H, Franzini E, Hakim J, Pasquier C. Mechanism of lysozyme inactivation and degradation by Iron. Arch Biochem Biophys. 1992 Nov 15;299(1):172–8.
8. Niki E, Saito M, Yoshikawa Y, Yamamoto Y, Kamiya Y. Oxidation of lipids. XII. Inhibition of oxidation of soybean phosphatidylcholine and methyl linoleate in aqueous dispersions by uric acid. Bull Chem Soc Jpn. 1986;59:471–7.
9. Niki E. Free radical initiators as source of water- or lipid-soluble peroxyl radicals. Methods Enzymol. 1990;186:100–8.
10. Ji JA, Zhang B, Cheng W, Wang YJ. Methionine, tryptophan, and histidine oxidation in a model protein, PTH: Mechanisms and stabilization. J Pharm Sci. 2009 Dec;98(12):4485–500.
11. Hawe A, Wiggenhorn M, van de Weert M, Garbe JHO, Mahler H, Jiskoot W. Forced Degradation of Therapeutic Proteins. J Pharm Sci. 2012 Mar;101(3):895–913.
12. Arenas A, López-Alarcón C, Kogan M, Lissi E, Davies MJ, Silva E. Chemical Modification of Lysozyme, Glucose 6-Phosphate Dehydrogenase, and Bovine Eye Lens Proteins Induced by Peroxyl Radicals: Role of Oxidizable Amino Acid Residues. Chem Res Toxicol. 2013 Jan 18;26(1):67–77.
13. Blake CC, Koenig DF, Mair GA, North AC, Philips DC, Sarma VR. Structure of hen egg-white lysozyme. A three-dimensional Fourier synthesis at 2 Angstrom resolution. Nature. 1965;206:757–61.
14. Pace CN, Vajdos F, Fee L, Grimsley G, Gray T. How to measure and predict the molar absorption coefficient of a protein. Protein Sci. 1995;4(11):2411–2423.
15. Rezwan K, Meier LP, Gauckler LJ. A Prediction Method for the Isoelectric Point of Binary Protein Mixtures of Bovine Serum Albumin and Lysozyme Adsorbed on Colloidal Titania and Alumina Particles. Langmuir. 2005 Apr;21(8):3493–7.
16. Canfield RE, Liu AK. The disulfide bonds of egg white lysozyme (muramidase). J Biol Chem. 1965;240(5):1997–2002.
17. da Silva Aquino KA. Sterilization by gamma irradiation [Internet]. INTECH Open Access Publisher; 2012 [cited 2016 May 14]. Available from: http://cdn.intechopen.com/pdfs/32842/InTech-Sterilization_by_gamma_irradiation.pdf

18. Chao C-C, Ma Y-S, Stadtman ER. Modification of protein surface hydrophobicity and methionine oxidation by oxidative systems. Proc Natl Acad Sci. 1997;94(7):2969–2974.
19. Liu H, Gaza-Bulseco G, Faldu D, Chumsae C, Sun J. Heterogeneity of Monoclonal Antibodies. J Pharm Sci. 2008 Jul;97(7):2426–47.
20. Kim B-H, Choi NH, Ok JH. Comparison of reversed-phase liquid chromatographic methods for the separation of new quinolones. J Chromatogr Sci. 2002;40(7):369–376.
21. Wyndham KD, O'Gara JE, Walter TH, Glose KH, Lawrence NL, Alden BA, et al. Characterization and Evaluation of C $_{18}$ HPLC Stationary Phases Based on Ethyl-Bridged Hybrid Organic/Inorganic Particles. Anal Chem. 2003 Dec;75(24):6781–8.
22. Van Deemter JJ, Zuiderweg FJ, Klinkenberg A. Longitudinal diffusion and resistance to mass transfer as causes of nonideality in chromatography. Chem Eng Sci. 1956;5:271–89.
23. Brune D, Kim S. Predicting protein diffusion coefficients. Proc Natl Acad Sci. 1993;90(9):3835–3839.
24. Bertini J, Mannucci C, Noferini R, Perico A, Rovero P. Rapid Simultaneous Determination of Tryptophan and Tyrosine in Synthetic Peptides by Derivative Spectroscopy. J Pharm Sci. 1993;82(2):179–82.
25. Nakazawa M, Manabe K. The Direct Hydrolysis of Proteins Containing Tryptophan on Polyvinylidene Difluoride Membranes by Mercaptoethanesulfonic Acid in the Vapor Phase. Anal Biochem. 1992;206(1):105–8.
26. Sultana N, Arayne MS, Khan MM, Saleem DM, Mirza AZ. Determination of Tryptophan in Raw Materials, Rat Brain and Human Plasma by RP-HPLC Technique. J Chromatogr Sci. 2012 Jul 1;50(6):531–7.
27. Shaked Z 'ev, Szajewski R, Whitesides G. Rates of Thiol-Disulfide Interchange Reactions Involving Proteins and Kinetic Measurements of Thiol pKa Values. Biochemistry (Mosc). 1980;19:4156–66.
28. Yokota A, Izutani K, Takai M, Kubo Y, Noda Y, Koumoto Y, et al. The transition state in the folding-unfolding reaction of four species of three-disulfide variant of hen lysozyme: the role of each disulfide bridge. J Mol Biol. 2000;295(5):1275–1288.
29. Chang J-Y, Li L. The unfolding mechanism and the disulfde structures of denatured lysozyme. FEBS Lett. 2002;511:73–8.
30. Wahl R, Zeng L, Madison S, DePinto R, Shay B. Mechanistic studies on the decomposition of water soluble azo-radical-initiators. J Chem Soc Perkin Trans. 1998;2(9):2009–18.
31. Barb WG, Baxendale JH, George P, Hargrave KR. Reactions of ferrous and ferric ions with hydrogen peroxide. Part I.—The ferrous ion reaction. Trans Faraday Soc. 47:462–500.
32. Rachmilovich-Calis S, Masarwa A, Meyerstein N, Meyerstein D, van Eldik R. New Mechanistic Aspects of the Fenton Reaction. Chem - Eur J. 2009 Aug 17;15(33):8303–9.
33. Pantopoulos K, Schipper H. Principles of Free Radical Biomedicine. Volume I. 1st ed. Vol. 1. Nova Science Publishers Inc; 2012. 328 p.
34. Singer PC. Anaerobic control of phosphate by ferrous iron. J Water Pollut Control Fed. 1972;663–669.
35. Lopalco A, Dalwadi G, Niu S, Schowen RL, Douglas J, Stella VJ. Mechanism of Decarboxylation of Pyruvic Acid in the Presence of Hydrogen Peroxide. J Pharm Sci. 2016 Feb;105(2):705–13.

APPENDICES

Appendix A: Definition & Abbreviation

Hydroxyl radical: HO•

Peroxyl radical: ROO•

Hydroperoxyl radical: HOO•

Superoxide radical: $\bullet O_2^-$

Hydroxyl anion: HO^-

G-Value: The number of species formed or destroyed per 100eV of energy absorbed

Gamma Irradiation: The process of exposing the product to gamma rays, the source of ionizing radiation.

Ionizing radiation: The type of radiation that has enough energy to remove electrons from the atom.

eV: electronvolt = 1.6022×10^{-19} joules

MeV: megaelectronvolt = 1.6022×10^{-13} joules

mCi: millicurie = 3.7×10^7 decays per second or becquerels

Ci: curie = 3.7×10^{10} decays per second or becquerels

MCi: megacurie = 3.7×10^{16} decays per second or becquerels

SAL: Sterility Assurance Level

RP: Reversed phase

HPLC: High Performance Liquid Chromatography

UPLC: Ultra Performance Liquid Chromatography

SEC: Size Exclusion Chromatography

ROS: Reactive Oxygen Species